Stellenbosch
UNIVERSITY
IYUNIVESITHI
UNIVERSITEIT

Full State Pose Estimation Using a Satellite Imager

by

D.P. Theron

Dissertation presented for the degree of Masters of (Electronic Engineering) in the Faculty of Engineering at Stellenbosch University

Supervisor: Prof. H.W. Jordaan
Dr. S. Busch

2025

To God, my Wife and my Mother

Acknowledgements

- Prof. H.W. Jordaan, thank you for all your patience and guidance trough this journey.
- Pinkmatter for your financial support for taking the risk of investing in me and my future. I will be enternally grateful. Thank you for letting me feel like part of the company and taking such good care of me during the visits.
- Clarissa, my wife, thank you for all your love and support during the difficult times.
- My Mother, words cannot describe how much you meant to me during my masters degree.
- My friend and collogues in the ESL, especially Brandon Chetty, Dane Groves and Mark Msonko, who put up with my 'new productivity hacks' and 'crazy ideas', but also keeping me on track.
- God, for all your guidance, support, love and faith in me, even though I didn't deserve it.

"*Whether you think you can or you can't, you're right.*"
– Mr. Henry Ford

Declaration

By submitting this dissertation electronically, I declare that the entirety of the work contained therein is my own, original work, that I am the sole author thereof (save to the extent explicitly otherwise stated), that reproduction and publication thereof by Stellenbosch University will not infringe any third party rights and that I have not previously in its entirety or in part submitted it for obtaining any qualification.

Date: 1 September 2025

Abstract

Pose estimation on nanosatellites is still an on going topic of interest. It is important for satellite to know there position and attitude to do accurate target tracking. Traditional solutions to the pose estimation problem is mainly star trackers, which looks at the constalations of stars to determine the attitude and GPS to determine the position of the satellite along with other sensors like magnetometers and coarse sun sensors.

In this thesis, a sensor is developed that utilises the onboard satellite imager, to estimate the position and the attitude of the satellite. The sensor uses a camera model to take pictures of the Earth surface, a feature detector is ran on the image using scale invariant feature transform (SIFT) to identify and establish corrospondance of features. A full state kinematic estimator using the extended Kalman Filter (EKF) based on the simultanous localisation and mapping (SLAM) approach. The filter makes used of feature vectors and feature discripters detected on the image. This is used to estimate attitude and position of the satellite.

An simulation environment in MATLAB is developed to propagate a satellite and determine the ground truth pose. Several traditional sensors like the star tracker and magnetometer and GPS to be able to compare the Earth Tracker and create the possiblity to fuse the sensors and determine the accuracy. Results show that the filter estimates the system states successfully. It is concluded that . . .

Uittreksel

Table of Contents

List of Figures

List of Tables

Nomenclature

Variables and Functions

Constants

ω_e	Rotation speed of the Earth
c	A constant.

Functions

f	A function.

Variables

$\mathbf{x}$	A variable.

Acronyms and Abbreviations

ADCS Attitude Determinination and Control System

BRF Body Refrence Frame

CRF Camera Reference Frame

DCM Direction Cosine Matrix

ECEF Earth Centred Earth Fixed

ECI Earth Centred Inertial

EKF Extended Kalman Filter

GPS Global Positioning System

LLA Lattitude Longitude and Altitude Reference Frame

LVLH Local Vertical Local Horizon

SLAM Simultanous Localisation and Mapping

Definitions

A

Attitude The orientation of a satellite in space.

P

Pose The combination of a satellite's position and attitude.

S

State Estimation The ability to determine a state of a system using mathematical models.

Student is an entity needing a thesis to transcend the state of being a student.

Variables and Functions

Constants

ω_e	Rotation speed of the Earth
c	A constant.

Functions

f	A function.

Variables

$\mathbf{x}$	A variable.

Chapter 1

Introduction

1.1 Problem Background

- Satellites are getting smaller - Because this leads to stallites having reduced costs and timelines - This is enables by the miniraturisation of electronics

- One of the big industires in satellites is remote sensing - Remote Sening is the application where satellites are used to monitor the Earth - One of the applications is to take images of the Earth

- This leads to the problem that high accuracy is needed to take images of the targets on the Earth's surface - COTS components which is mainly used on small satellites lack the accuracy needed - Magnetometers is to low of an accuracy - Star Trackers have the right accuracy, but is expensive

1.2 Problem Defintion

A satellite orbiting Earth in the Earth-Centered Inertial (ECI) reference frame performs Earth observation missions, continuously capturing high-resolution imagery of the planet's surface for scientific, commercial, or operational purposes. To fulfill mission objectives effectively, the satellite must provide not only high-quality imagery but also precise geographic information about observed areas. This requires accurate knowledge of the satellite's six-degree-of-freedom pose (three-dimensional position and three-dimensional attitude) relative to the ECI frame at the moment each image is captured.

Traditional satellite pose determination relies on external systems such as Global Navigation Satellite Systems (GNSS) and ground-based tracking networks. However, this thesis investigates an autonomous approach where the satellite performs "visual navigation" by identifying known ground features in its imagery and using these observations to determine its orbital state. The satellite essentially performs "reverse GPS" - instead of receiving position signals from space, it observes recognizable landmarks on Earth's surface and computes its pose from these visual references.

The core technical challenge lies in the transformation from raw imagery to precise pose estimates. This involves several interdependent problems: **(1) Feature Detection** - identifying which pixels in the imagery correspond to cataloged landmarks among millions of pixel observations; **(2) Geometric Inversion** - solving the complex inverse problem of determining six-dimensional pose from two-dimensional image projections of three-dimensional landmarks with known geographic coordinates; and **(3) Uncertainty Management** - handling measurement noise, feature detection errors, and dynamic orbital motion in real-time. This thesis assumes the availability of a pre-established catalog of ground features with precisely known geographic coordinates in the ECI frame. The feature matching problem - associating detected image features with specific catalog entries - is considered solved through prior knowledge of the observed terrain and existing geographic databases.

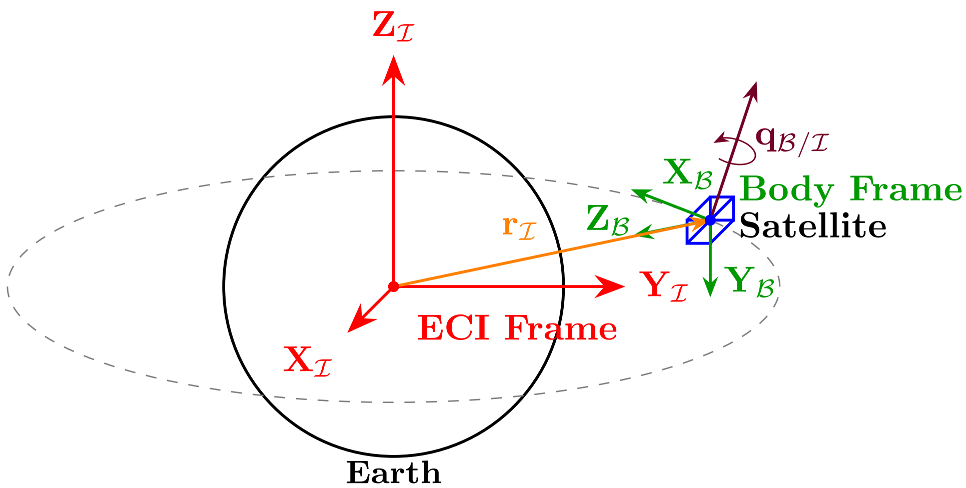

Figure 1.1: Satellite pose estimation concept showing orbital geometry, reference frames

This problem structure aligns with a simplified version of the Simultaneous Localization and Mapping (SLAM) framework. In this context, **localization** corresponds to determining the satellite's pose relative to the ECI frame using observations of cataloged features, while the **mapping** component is reduced to feature catalog utilization rather than creation. Since the geographic locations of observable features are assumed known a priori, the primary focus becomes the pose estimation problem given established feature correspondences.

The satellite's pose estimation system must account for the dynamic nature of orbital motion, the geometric relationship between the camera frame and satellite body frame, and the projection characteristics of the imaging system, while maintaining computational efficiency suitable for real-time onboard processing.

1.3 Proposed Solution

- Proposed solution is to develop an estimation algorithm that can estimate the full state of the satellite - The Full State of a Satellite is its postition in Space and its attitude or its orientation in space. - The satellite uses the imager itself to determine position and attitude. - This can lead to reduce costs as the satellite is using an instrument which is already onboard the satellite. - Utilising the components when it is idle - Observing the target directly

1.4 Document Outline

- Chapter 2: Wil investigate previous sensors that is being used to determine Propose - Previous techniques estimating the pose - Some light touching on feature detection as this is crucial to the pose estimation system

- Chapter 3: Wil introduce the modelling of the system - Rigid Body Kinematics - Position Kinematics - Attitude Kinematics - Kalman Filters - Extended Kalman Filters

- Chapter 4: Measurement Generation - Feature detection - PinHole Camera Model. - The Plant - The Plant Model - The Measurment Model

- Chapter 5: State estimation - The Extended Kalman Filter - Update Step - Prediction Step - Simulator

- Chapter 6 is results

- Chapter 7 is Conclusion - Future Work

Chapter 2

Literature

2.1 Introduction

Chapter 3

Modelling

3.1 Introduction

To accurately describe the full pose of a satellite using an onboard imaging system, a comprehensive mathematical model of the spacecraft must be established. This chapter presents the fundamental modeling framework required for vision-based satellite pose estimation. The chapter begins by defining the core problem and establishing the system requirements for satellite pose determination. Subsequently, the kinematic and dynamic equations governing satellite motion are derived, providing the mathematical foundation for state propagation. The various reference frames utilized throughout this work are systematically defined, including the transformations necessary to relate measurements and states across different coordinate systems. Additionally, this chapter presents the mathematical models for the accompanying sensors integrated within the pose estimation system. These sensor models are essential for the multi-sensor fusion approach employed in the Extended Kalman Filter implementation presented in later chapters.

3.2 Rigid Body Mechanics

3.2.1 Kinematics

The pose of a rigid body within a reference frame encompasses both its spatial position and angular orientation. The attitude describes the rotational relationship between the body-fixed coordinate system and a known reference coordinate system. This rotational relationship is typically expressed through a rotation matrix, commonly known as a direction cosine matrix (DCM).[1][2][3][4], Elementary rotations around individual coordinate axes are termed coordinate rotations. The fundamental coordinate rotations about the x-, y-, and z-axes, characterized by rotation angles ϕ, θ, and ψ respectively, can be mathematically expressed as

$$R_x(\phi) = \begin{bmatrix} 1 & 0 & 0 \\ 0 & \cos(\phi) & \sin(\phi) \\ 0 & -\sin(\phi) & \cos(\phi) \end{bmatrix} \tag{3.1}$$

$$R_y(\theta) = \begin{bmatrix} \cos(\theta) & 0 & -\sin(\theta) \\ 0 & 1 & 0 \\ \sin(\theta) & 0 & \cos(\theta) \end{bmatrix} \tag{3.2}$$

$$R_z(\psi) = \begin{bmatrix} \cos(\psi) & \sin(\psi) & 0 \\ -\sin(\psi) & \cos(\psi) & 0 \\ 0 & 0 & 1 \end{bmatrix} \tag{3.3}$$

Any rotation in 3D space can be described by three coordinate rotations. The DCM describing the rotation from the orbital reference frame $\mathcal{O}$ to the body reference frame $\mathcal{B}$, $\mathbf{A}_{\mathcal{O}}^{\mathcal{B}}$, can be represented by three Eular angles. Each of the angles corresponds to one coordinate rotation. The order of the Eular 1-2-3 or a Roll, Ptich, Yaw rotation, shown in Figure 3.5, is expressed as

$$\boldsymbol{A}_{\mathcal{O}}^{\mathcal{B}} = R_x(\phi)R_y(\theta)R_z(\psi) \tag{3.4}$$

$$\begin{bmatrix} a_{1,1} & a_{1,2} & a_{1,3} \\ a_{2,1} & a_{2,2} & a_{2,3} \\ a_{3,1} & a_{3,2} & a_{3,3} \end{bmatrix} \tag{3.5}$$

$$\begin{bmatrix} C\theta C\psi & C\theta S\psi & -S\theta \\ S\phi S\theta C\psi - C\phi S\psi & S\phi S\theta S\psi + C\phi C\psi & S\phi C\theta \\ C\phi S\theta C\psi + S\phi S\psi & C\phi S\theta S\psi - S\phi C\psi & C\phi C\theta \end{bmatrix} \tag{3.6}$$

Where S is the sine function and C is the cosine function. The Eular angles are calculated as follows

$$\phi = \arctan 2 \left(\frac{a_{2,3}}{a_{3,3}} \right) \tag{3.7}$$

$$\theta = \arctan 2 \left(\frac{-a_{1,3}}{\sqrt{a_{1,1}^2} + \sqrt{a_{1,2}^2}} \right) \tag{3.8}$$

$$\psi = \arctan 2 \left(\frac{a_{1,2}}{a_{1,1}} \right) \tag{3.9}$$

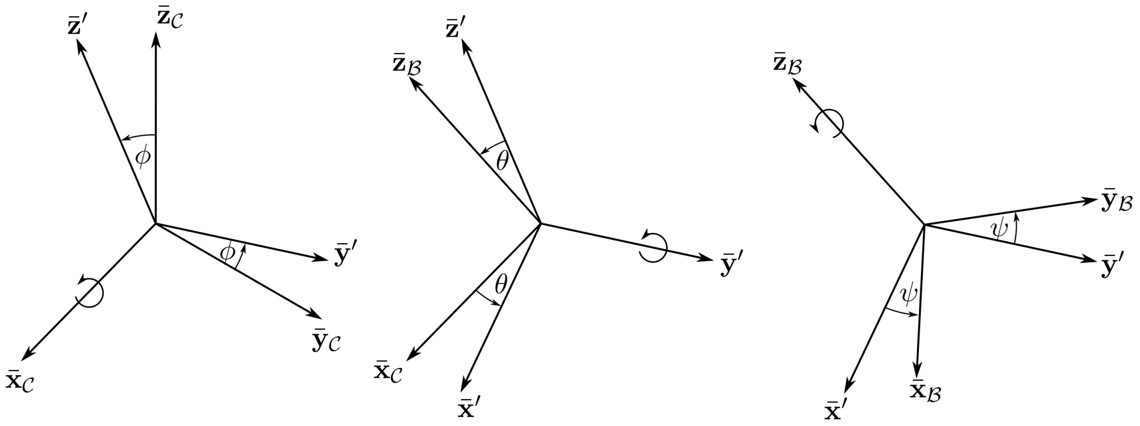

Figure 3.1: Eular 1-2-3 Rotation[1]

Mathematicl singularities occur when using Eular angles to represent large rotations. When both $a_{1,1}$ and $a_{1,2}$ in Equation3.4 are zero, the expressions for ψ and θ are undefined. This is known as *gimbal lock*, where the changes in the first and third Eular angles are indistinguishable when the second angle nears a criticual value. Alternatively, the DCM can be described using quaternions, which do not have these singularities. The quaternion rotation is Figure3.1 is expressed by the Eular axis $\bar{\mathbf{e}} = [e_x, e_y, e_z]^T$ and the angle θ

$$\mathbf{q} = \begin{bmatrix} q_s \\ q_x \\ q_y \\ q_z \end{bmatrix} = \begin{bmatrix} \cos(\theta/2) \\ e_x \sin(\theta/2) \\ e_y \sin(\theta/2) \\ e_z \sin(\theta/2) \end{bmatrix} \tag{3.10}$$

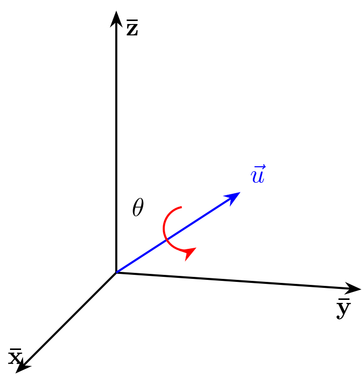

Figure 3.2: Quaternion Rotation

The DCM as a function of Quaternion set is expressed as,

$$\mathbf{A}_{\mathcal{O}}^{\mathcal{B}} = \begin{bmatrix} q_s^2 + q_x^2 - q_y^2 - q_z^2 & 2(q_xq_y - q_sq_z) & 2(q_xq_z + q_sq_y) \\ 2(q_xq_y + q_sq_z) & q_s^2 - q_x^2 + q_y^2 - q_z^2 & 2(q_yq_z - q_sq_x) \\ 2(q_xq_z - q_sq_y) & 2(q_yq_z + q_sq_x) & q_s^2 - q_x^2 - q_y^2 + q_z^2 \end{bmatrix} \tag{3.11}$$

Using the normalisation constraint, $q_s^2 + q_x^2 + q_y^2 + q_z^2 = 1$, the DCM Simplifies to,

$$\mathbf{A}_{\mathcal{O}}^{\mathcal{B}} = \begin{bmatrix} 1 - 2(q_y^2 + q_z^2) & 2(q_xq_y - q_sq_z) & 2(q_xq_z + q_sq_y) \\ 2(q_xq_y + q_sq_z) & 1 - 2(q_x^2 + q_z^2) & 2(q_yq_z - q_sq_x) \\ 2(q_xq_z - q_sq_y) & 2(q_yq_z + q_sq_x) & 1 - 2(q_x^2 + q_y^2) \end{bmatrix} \tag{3.12}$$

The body-fixed angular rates of the satellite in ORB, $\omega_{\mathcal{B}/\mathcal{O}}$, is expressed as a function of qauternions by,

$$\omega_{\mathcal{B}/\mathcal{O}} = \begin{bmatrix} \omega_{bx} \\ \omega_{by} \\ \omega_{bz} \end{bmatrix} = 2 \begin{bmatrix} -q_x & q_s & -q_z & q_y \\ -q_y & q_z & q_s & -q_x \\ -q_z & -q_y & q_x & q_s \end{bmatrix} \begin{bmatrix} \dot{q}_s \\ \dot{q}_x \\ \dot{q}_y \\ \dot{q}_z \end{bmatrix} \tag{3.13}$$

Inversly the quaternion rates as a function of the body rates are,

$$\begin{bmatrix} \dot{q}_s \\ \dot{q}_x \\ \dot{q}_y \\ \dot{q}_z \end{bmatrix} = \frac{1}{2} \begin{bmatrix} 0 & -\omega_{bx} & -\omega_{by} & -\omega_{bz} \\ \omega_{bx} & 0 & \omega_{bz} & -\omega_{by} \\ \omega_{by} & -\omega_{bz} & 0 & \omega_{bx} \\ \omega_{bz} & \omega_{by} & -\omega_{bx} & 0 \end{bmatrix} \begin{bmatrix} q_s \\ q_x \\ q_y \\ q_z \end{bmatrix} \tag{3.14}$$

Throughout this thesis, quaternions serve as the primary attitude representation method. Quaternions eliminate rotational sequence ambiguities and define rotations about a clearly specified axis. The trigonometric components of the rotation matrix are inherently embedded within the quaternion-based DCM formulation. Consequently, attitude transformations require only a single matrix operation using quaternions, whereas Euler angle representations necessitate three separate operations.

3.2.2 Dynamics

3.2.2.1 Translational Dynamics

For the translational dynamics, Newton's second law governs the linear motion of the satellite with mass m. The discrete-time position and velocity propagation equations are:

$$\mathbf{r}_t = \mathbf{r}_{t-1} + \mathbf{v}_t\Delta t + \frac{1}{2m}\mathbf{F}(t)\Delta t^2 \tag{3.15}$$

$$\mathbf{v}_t = \mathbf{v}_{t-1} + \frac{1}{m}\mathbf{F}(t)\Delta t \tag{3.16}$$

where **F** denotes the resultant external force applied to the satellite. Within the orbital regime examined in this study, external disturbances are considered insignificant relative to gravitational effects. Additionally, given the potential unavailability of precise mass characteristics, the translational dynamics may be adequately represented through kinematic approximations wherein the instantaneous velocity is predominantly governed by the preceding velocity state.

In orbital mechanics, the gravitational force **F** acting on a spacecraft is proportional to its position vector **r** relative to the center of mass. This force is described by the following equation, where $\boldsymbol{\mu}$ denotes Earth's gravitational parameter:

$$\ddot{\mathbf{r}} = \mathbf{F}\mathbf{u}_r \tag{3.17}$$

$$\ddot{\mathbf{r}} = \frac{-\mu}{||\mathbf{r}||^3}\mathbf{u}_r \tag{3.18}$$

The acceleration of a spacecraft in orbit is influenced by several factors, including the primary gravitational force $\mathbf{F}_G$, the J_2 perturbation $\mathbf{F}_{J2}$, atmospheric drag $\mathbf{F}_{\text{drag}}$, solar radiation pressure $\mathbf{F}_{\text{sol}}$, and other miscellaneous perturbations $\mathbf{F}_{\text{misc}}$.

The total force acting on the satellite can therefore be expressed as:

$$\mathbf{F}_{total} = \mathbf{F}_G + \mathbf{F}_{J2} + \mathbf{F}_{drag} + \mathbf{F}_{sol} + \mathbf{F}_{misc} \tag{3.19}$$

However, since we are only modeling Low Earth Orbits (LEO) over a short time period, only the primary gravitational force $\mathbf{F}_G$ and the J_2 perturbation $\mathbf{F}_{J2}$ are considered.
The J_2 perturbation, which accounts for the Earth's oblateness, is modeled in the Earth-Centered Inertial (ECI) frame using the following equation:

$$\mathbf{a}_{J2} = \frac{3}{2} * J_2 * \frac{\mu R_E}{||\mathbf{r}||^5} \begin{bmatrix} r_x(1 - 5\frac{z^2}{r^2}) \\ r_y(1 - 5\frac{z^2}{r^2}) \\ r_z(3 - 5\frac{z^2}{r^2}) \end{bmatrix} \tag{3.20}$$

In this equation, μ represents Earth's gravitational parameter, R_E is the mean radius of the Earth, J_2 is the second zonal harmonic coefficient accounting for the Earth's oblateness, and **r** denotes the satellite's position vector expressed in the Earth-Centered Inertial (ECI) frame.

3.2.2.2 Rotational Dynamics

The rotational dynamics of a rigid satellite are governed by the Newton-Euler equations, which apply to all rigid inertial bodies. The angular momentum **H** of the satellite is expressed as:

$$\dot{\mathbf{H}} = \frac{d\mathbf{H}}{dt} = \mathbf{I}\dot{\boldsymbol{\omega}} \tag{3.21}$$

where $\mathbf{H}$ is the angular momentum vector, $\boldsymbol{\omega}$ is the angular velocity vector expressed in the body frame, and $\mathbf{I}$ is the diagonalized moment of inertia tensor about the satellite's principal axes.

In the absence of external torques, the rotational motion about the satellite's center of mass can be described by Euler's equations:

$$I_{xx}\dot{\omega}_x = \omega_y\omega_z(I_{yy} - I_{zz}) \tag{3.22}$$

$$I_{yy}\dot{\omega}_y = \omega_x\omega_z(I_{zz} - I_{xx}) \tag{3.23}$$

$$I_{zz}\dot{\omega}_z = \omega_x\omega_y(I_{xx} - I_{yy}) \tag{3.24}$$

where I_{xx}, I_{yy}, and I_{zz} are the principal moments of inertia, which are constant and determined by the satellite's mass distribution and geometry.

The stability of the satellite's rotational motion is influenced by its moment of inertia. According to Marsden and Ratiu, rotation about the major or minor principal axis is stable, while rotation about the intermediate axis is inherently unstable. Under constant energy conditions, any initial rotation around the intermediate axis will tend to redistribute energy toward the major and minor axes due to nutation effects.

To propagate the satellite's attitude over time, the quaternion derivative must be computed. The quaternion $\mathbf{q}_{B/I}$, which represents the rotation from the inertial frame to the body frame, evolves according to:

$$\dot{\mathbf{q}}_{B/I} = \frac{1}{2}(\mathbf{q}_{B/I} \otimes \boldsymbol{\omega}) \tag{3.25}$$

where $\boldsymbol{\omega} = [\omega_x, \omega_y, \omega_z]^T$ is the angular velocity vector in the body frame, and $\otimes$ denotes quaternion multiplication. Expanding this yields:

$$\dot{\mathbf{q}}_{B/I} = \frac{1}{2}\begin{bmatrix} q_{B/I,0}\omega_x - q_{B/I,3}\omega_y + q_{B/I,2}\omega_z \\ q_{B/I,3}\omega_x + q_{B/I,0}\omega_y - q_{B/I,1}\omega_z \\ -q_{B/I,2}\omega_x + q_{B/I,1}\omega_y + q_{B/I,0}\omega_z \\ -q_{B/I,1}\omega_x - q_{B/I,2}\omega_y - q_{B/I,3}\omega_z \end{bmatrix} \tag{3.26}$$

where $q_{B/I,0}$ is the scalar part and $q_{B/I,1}, q_{B/I,2}, q_{B/I,3}$ are the vector components of the quaternion.

Quaternion propagation is performed using a simple Euler integration scheme. First, the quaternion is advanced in time as:

$$\bar{\mathbf{q}}_{B/I}(t+\Delta t) = \mathbf{q}_{B/I}(t) + \dot{\mathbf{q}}_{B/I}\Delta t \tag{3.27}$$

where $\bar{\mathbf{q}}_{B/I}$ is the unnormalized quaternion. To maintain a valid attitude representation, the quaternion must be renormalized:

$$\mathbf{q}_{B/I}(t+\Delta t) = \frac{\bar{\mathbf{q}}_{B/I}(t+\Delta t)}{||\bar{\mathbf{q}}_{B/I}(t+\Delta t)||} \tag{3.28}$$

This normalization step ensures that the quaternion maintains unit magnitude throughout integration.

3.3 Refrence Frame Transformations

In this project, several different reference frames will be encountered. To accurately construct the measurement model, it is essential to understand each of these reference frames and the transformations between them.

3.3.1 Transformation Matrix

Transformations between different reference frames are a fundamental part of spacecraft modeling and sensor simulation. These transformations are typically expressed using homogeneous transformation matrices, which combine both rotation and translation components into a single 4×4 matrix.

3.3.1.1 Rotation Matrix

In many practical scenarios, such as pure attitude transformations or body-to-inertial frame conversions, only rotational alignment is needed. In such cases, only the DCM $\mathbf{A}$ is used like discussed in previous chapters, and the transformation is defined as:

$$\mathbf{v}_{\mathcal{O}} = \mathbf{A}_{\mathcal{I}}^{\mathcal{O}} \cdot \mathbf{v}_{\mathcal{I}} \tag{3.29}$$

Note that:

$$\mathbf{A}_{\mathcal{I}}^{\mathcal{O}} = \left(\mathbf{A}_{\mathcal{O}}^{\mathcal{I}}\right)^{\top} \tag{3.30}$$

and that the reverse rotation can be applied.

$$\mathbf{v}_{\mathcal{I}} = \left(\mathbf{A}_{\mathcal{I}}^{\mathcal{O}}\right)^{T} \cdot \mathbf{v}_{\mathcal{O}} \tag{3.31}$$

This relationship arises because direction cosine matrices are orthogonal.

3.3.1.2 Translation

In many of the reference frames the translation of the origin is required, To translate from one refrence frame the the other

$$\mathbf{v}_{\mathcal{B}/\mathcal{I}} = \mathbf{v}_{\mathcal{B}} - \mathbf{r}_{\mathcal{I}} \tag{3.32}$$

Where $\mathbf{v}_{\mathcal{B}/\mathcal{I}}$ is the vector in $\mathcal{B}$ relative to $\mathcal{I}$ and $\mathbf{v}_{\mathcal{B}}$ is the vector in the body frame and $\mathbf{r}_{\mathcal{I}}$ is the position of the Body frame origin in the inertial reference frame.

3.3.1.3 Homogeneous Transformation Matrix

A homogeneous transformation matrix from $\mathcal{I}$ to $\mathcal{O}$ is defined as:

$$\mathbf{T}_{\mathcal{I}}^{\mathcal{O}} = \begin{bmatrix} \mathbf{A}_{\mathcal{I}}^{\mathcal{O}} & -\mathbf{A}_{\mathcal{I}}^{\mathcal{O}} \cdot \mathbf{r}_{\mathcal{I}} \\ \mathbf{0}_{1\times 3} & 1 \end{bmatrix} \tag{3.33}$$

Here, $\mathbf{A}_{\mathcal{I}}^{\mathcal{O}}$ is a 3×3 direction cosine matrix (DCM) that describes the orientation of frame $\mathcal{O}$ relative to frame $\mathcal{I}$, and $\mathbf{r}_{\mathbf{I}}$ is a translation vector from the origin of $\mathcal{I}$ to the origin of $\mathcal{O}$, expressed in frame $\mathcal{I}$.

This formulation ensures that both the direction and magnitude of vectors are preserved during the transformation. However, it is important to note that the inverse transformation is **not** obtained from getting the transpose.

$$\mathbf{T}_{\mathcal{I}}^{\mathcal{O}} \neq \left(\mathbf{T}_{\mathcal{O}}^{\mathcal{I}}\right)^{T} \tag{3.34}$$

3.3.2 Lattitude, longitude and altitude

The lattitude, longitude and altitude of a feature or the position of the satellite is donated with the $\mathcal{L}$. The lattitude of a feature is the position of how high or low it above the equator, having a range of $-90°$ to $90°$. The longitude is based of the greenwich maridian, a longitude line that pases through the north- and south pole, it has a range of $-180°$ to $180°$. The altitude is measured form the the "WGS84" elliptical globe.

$$\mathbf{r}_{\mathcal{L}} = \begin{bmatrix} \lambda \\ \phi \\ h \end{bmatrix} \tag{3.35}$$

3.3.3 Earth Cenetered Earth Fixed

The Earth Centered Earth Fixed also known as Earth Centered Rotating (ECR) refrence frame is represented by the $\mathcal{R}$ and is very simular to the $\mathcal{L}$ reference frame with the z-axis alligned with the northpole and the x-axis points at the crossing of the Prime Maridian an the Equator, where the y-axis completes the right hand rule. The x,y and z-axis is defined in kilometers. To covert from $\mathcal{L}$ to $\mathcal{R}$ is to use a "WGS84" transfomr. Where WGS84 stands for World Geodetic System 1984, which is the standard coordinate system used for Global Positioning System (GPS). The WGS84 transformation uses a reference ellipsoid that uses a semi-major axis of 6,378 km and a flatting of 1/298.2 .

$$\mathbf{T}_{\mathcal{L}}^{\mathcal{F}} = f(\mathrm{WGS84}) \tag{3.36}$$

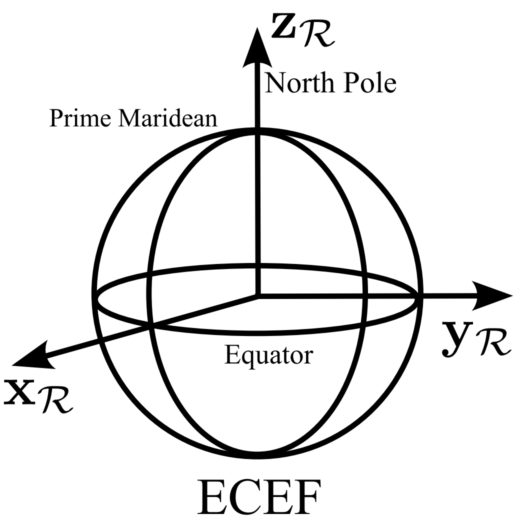

(a) The Earth-Centered, Earth-Fixed (ECEF) reference frame.

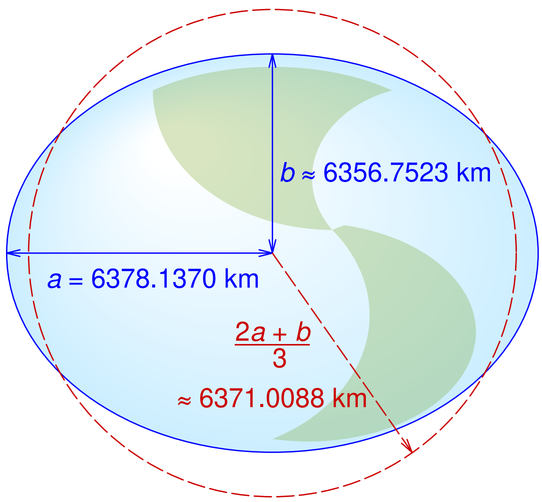

(b) WGS84 model showing the mean Earth radius.

Figure 3.3: Geodetic reference frames and models used in Earth observation.

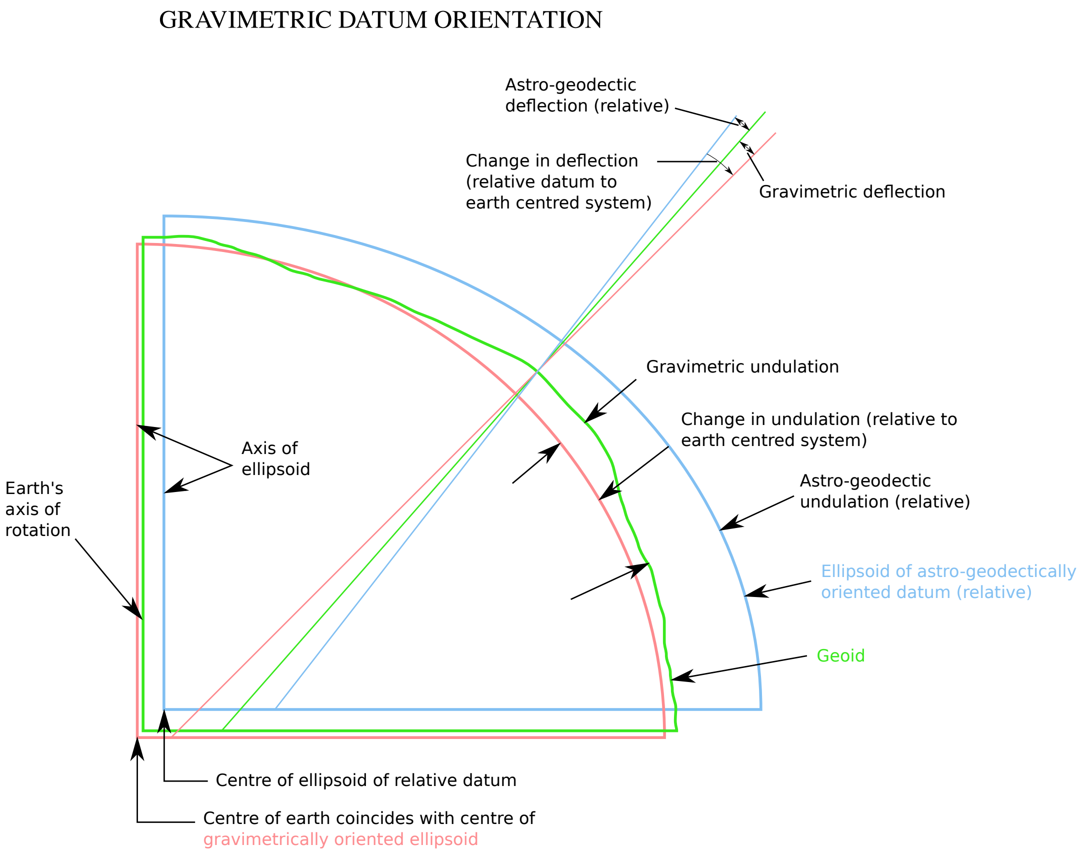

Figure 3.4: The Earth Cetred Earth Fixed reference frame

3.3.4 Earth Ceneterd Inertial

The Earth Centered Inertial refrence fream (ECI) refrenced by $\mathcal{I}$ shares a refrence frame axis with the ECEF, but is rotated about the z-axis. The Earth Centered refrence frame is defined as the x-axis pointing in the direction where the equatorial plane and the ecliptic plane cross, also known as the Vernal equanox, the z-axis is degined as the north pole and the Y axis completes the right hadn rule. This rotation is governed by the rotation speed of the earth ω_e which is 7.2921×10^{-5} rad/s and time t. To transform from the ECEF reference frame to the ECI reference frame one shouldrotate the Earth clockwise e.i.

$$\mathbf{A}_{\mathcal{F}}^{\mathcal{I}} = R(\omega_e t) = \begin{bmatrix} \cos(-\omega_e t) & -\sin(-\omega_e t) & 0 \\ \sin(-\omega_e t) & \cos(-\omega_e t) & 0 \\ 0 & 0 & 1 \end{bmatrix} \tag{3.37}$$

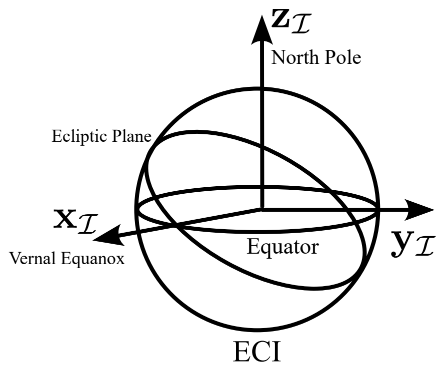

Figure 3.5: Earth Centered Earth Inertial Reference Frame

3.3.5 Orbital reference frame

The orbital reference frame used is the Local Vertical Local Horizon (LVLH) denoted by $\mathcal{O}$.The LVLH frame is a rotating, orbit-attached corrdinate system commonly used in spacecraft dynamics. It moves with the satellite and is defined relative to its orbit around Earth. The z-axis is the local vertical and is also called the Nadir direction, it points to the barycenter of the system, in this case the center of the Earth. The y-axis is called the cross track t points out of the orbital plane, typically the anti-angular momentum vector direction (anti-normal to the orbit plane). The x-axis is the "Local Horizon" also called "along track" pointing forward it is tangent to the orbit and completes the right hand rule.

If $\mathbf{r}$ is the position vector of the satellite and $\mathbf{v}$ is the velocity vector of the satellite. The equation for the reference frame is:

$$\bar{z}_{\mathcal{O}} = -\frac{\mathbf{r}}{||\mathbf{r}||} \tag{3.38}$$

$$\bar{y}_{\mathcal{O}} = \frac{\mathbf{r} \times \mathbf{v}}{||\mathbf{r} \times \mathbf{v}||} \tag{3.39}$$

$$\bar{x}_{\mathcal{O}} = \bar{y}_{\mathcal{O}} \times \bar{z}_{\mathcal{O}} \tag{3.40}$$

For this reference frame there should also be a refrence frame translation introduced. Which is done by substracing $\mathbf{r}$ from the vector

$$\mathbf{f}_{\mathcal{O}} = \mathbf{A}_{\mathcal{I}}^{\mathcal{O}} \times (\mathbf{f}_{\mathcal{I}} - \mathbf{r}_{\mathcal{I}}) \tag{3.41}$$

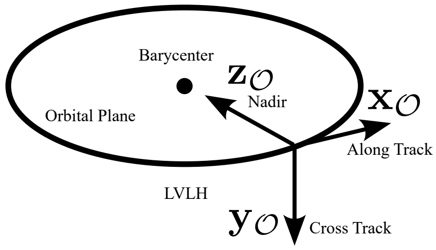

Figure 3.6: The Orbital Reference frame (also known as the LVLH)

3.3.6 Body Referenece frame

The body reference frame denoted by $\mathcal{B}$ is the reference frame of the satellite body itself, with the center point referenced as the center of mass of the satellite body. with the z-axis defined as the yaw, x-axis defined as the roll and the y-axis defined as the pitch of the satellite. With the body frame z-axis and the orbital reference frame as alligned at initialisiation

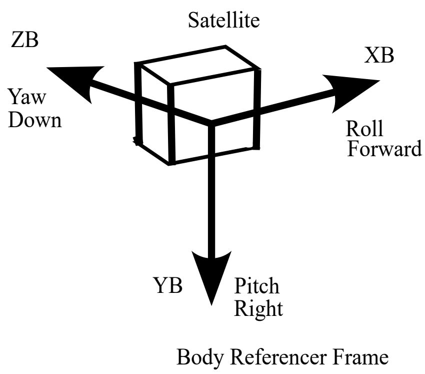

Figure 3.7

3.4 Sensor Modelling

3.4.1 GPS Measurement Model

In the simulation, GPS measurements are generated using the same underlying dynamics as the truth model, which is based on the two-body problem. This ensures consistency between the true satellite motion and the measurement framework. However, to emulate realistic sensor behavior, the GPS measurements are corrupted by both noise and drift.

One of the GPS sensor outputs is called $GPGGA which contains the tim, lattitude, longitude and altitude data. To model this measurement the simualted measurement $\mathbf{x}_{\text{true,pos}}$ needs to be converted to a the $\mathcal{L}$ representation

$$\mathbf{x}_{\text{true,pos},\mathcal{L}} = f(\text{WGS84}, \mathbf{A}_{\mathcal{I}}^{\mathcal{R}}, \mathbf{x}_{\text{true,pos},\mathcal{I}}) \tag{3.42}$$

The GPS measurement model is expressed as:

$$\mathbf{z}_{GPS}(t) = \mathbf{x}_{\text{true}}(t) + \boldsymbol{\eta}_{GPS}(t) + \mathbf{d}_{GPS}(t), \tag{3.43}$$

Let $\mathbf{z}_{GPS}(t)$ denote the observed GPS measurement at time t, which is modeled as the sum of the true system state $\mathbf{x}_{\text{true}}(t)$, as propagated by the two-body equations of motion, additive zero-mean Gaussian measurement noise $\boldsymbol{\eta}_{GPS}(t)$, and a GPS drift component $\mathbf{d}_{GPS}(t)$.

The drift component models the slow, unbounded accumulation of error that is characteristic of certain classes of low-cost GPS receivers. It is implemented as a random walk process:

$$\mathbf{d}_{GPS}(t) = \mathbf{d}_{GPS}(t - \Delta t) + \mathbf{q}_{GPS}(t), \tag{3.44}$$

Here, $\mathbf{d}_{GPS}(t - \Delta t)$ represents the GPS drift at the previous timestep, and $\mathbf{q}_{GPS}(t)$ is a zero-mean stochastic increment that models the drift rate. This increment is typically drawn from a Gaussian distribution, given by

$$\mathbf{q}_{GPS}(t) \sim \mathcal{N}(0, \sigma_d^2 \mathbf{I}). \tag{3.45}$$

This formulation captures both short-term measurement variability through $\boldsymbol{\eta}_{GPS}(t)$ and long-term bias trends via $\mathbf{d}_{GPS}(t)$, allowing for more realistic testing and evaluation of estimation algorithms under degraded or imperfect sensing conditions.

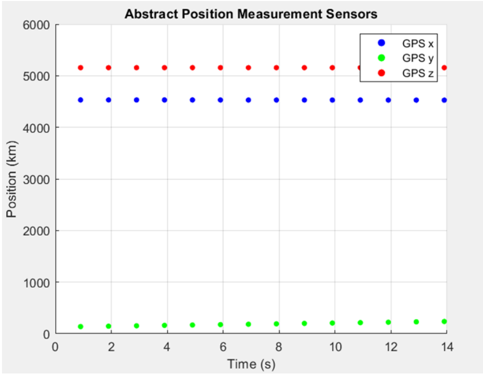

Figure 3.8

Insert Image of Modelled GPS Results

3.4.2 Gyroscope Measurement Model

The gyroscope provides a measurement of the angular velocity of the body frame relative to the inertial frame, expressed in the body frame. This quantity is denoted as $\boldsymbol{\omega}^B_{B/I}$, and forms a critical part of attitude determination and estimation systems.

To simulate a realistic sensor, the gyroscope measurement is corrupted by both random noise and a time-varying bias, or drift. The measurement model is given by:

$$\mathbf{z}_{\text{Gyro}}(t) = \boldsymbol{\omega}^B_{B/I}(t) + \boldsymbol{\eta}_{\text{Gyro}}(t) + \mathbf{d}_{\text{Gyro}}(t), \tag{3.46}$$

where:

- $\mathbf{z}_{\text{Gyro}}(t)$ is the observed gyroscope measurement at time t,
- $\boldsymbol{\omega}^B_{B/I}(t)$ is the true angular velocity of the body frame relative to the inertial frame,
- $\boldsymbol{\eta}_{\text{Gyro}}(t)$ is zero-mean Gaussian noise representing short-term measurement error, and
- $\mathbf{d}_{\text{Gyro}}(t)$ is the gyroscope drift, modeled as a time-varying bias.

The drift is modeled as a random walk process, capturing slow variations in the sensor bias over time:

$$\mathbf{d}_{\text{Gyro}}(t) = \mathbf{d}_{\text{Gyro}}(t - \Delta t) + \mathbf{q}_{\text{Gyro}}(t), \tag{3.47}$$

with the stochastic increment defined as:

$$\mathbf{q}_{\text{Gyro}}(t) \sim \mathcal{N}(0, \sigma_g^2 \mathbf{I}), \tag{3.48}$$

where σ_g^2 represents the drift rate variance of the gyroscope.

This model allows for the representation of both high-frequency noise and long-term integration drift, which are commonly observed in practical inertial measurement units (IMUs). Incorporating this model into the estimation framework enables more robust and accurate state reconstruction in the presence of sensor imperfections.

3.4.3 Star Tracker

The Star Tracker (ST) is a high-accuracy attitude sensor that provides an absolute measurement of the spacecraft's orientation, typically in quaternion form. Unlike relative sensors such as gyroscopes, the Star Tracker outputs an independent estimate of the spacecraft's attitude by capturing star field images and comparing them to a catalog.

In this simulation, the Star Tracker measurement is generated by perturbing the true attitude quaternion with a small random rotation. This models the sensor's measurement noise, which is assumed to follow a zero-mean Gaussian distribution.

Noise Quaternion Generation To simulate this noise, a small random rotation axis is sampled from a standard normal distribution and normalized. A noise quaternion $\mathbf{q}_{\text{noise}}$ is then constructed from this axis and a given angular noise magnitude θ (specified in degrees):

$$\mathbf{q}_{\text{noise}} = \begin{bmatrix} \cos\left(\frac{\theta}{2}\right) \\ \hat{\mathbf{u}} \sin\left(\frac{\theta}{2}\right) \end{bmatrix} \tag{3.49}$$

where $\hat{\mathbf{u}}$ is a unit vector sampled from $\mathcal{N}(0,1)^3$ and $\theta = \deg 2rad(ST_{\text{noise}})$.

Measurement Model The measured Star Tracker quaternion is computed by applying the noise quaternion to the true attitude quaternion using the Hamilton product:

$$\mathbf{z}_{ST} = \mathbf{q}_{\text{noise}} \otimes \mathbf{q}_{\text{true}} \tag{3.50}$$

This represents a small perturbation of the true attitude, emulating realistic sensor output.

This model captures the key behavior of a real Star Tracker by applying small rotational noise to the true spacecraft attitude. It is suitable for use in truth-model simulations and Kalman filter evaluations, providing high-fidelity yet controllable measurement uncertainty.

Add Some Results

3.4.4 Coarse Sun Sensor

The Coarse Sun Sensor (CSS) is a fundamental attitude sensing instrument in nanosatellite systems, providing an estimate of the Sun direction relative to the satellites body frame.

This subsection outlines the modeling approach for simulating CSS measurements, including the transformation of reference frames, sensor configuration, noise characteristics, and estimation logic.

Sun Vector in Inertial Frame The Sun vector is modeled in the Earth-Centered Inertial (ECI) frame as a fixed unit vector pointing in the $+X$ direction:

$$\mathbf{S}_{\mathcal{I}} = \begin{bmatrix} 1 & 0 & 0 \end{bmatrix}^\top \tag{3.51}$$

This simplified model assumes that the Sun direction does not vary during the simulation.

Transformation to Body Frame To simulate the Sun vector in the satellite's body frame, the inertial vector is rotated using the satellite's true attitude quaternion. The corresponding direction cosine matrix (DCM) is derived as:

$$\mathbf{S}_{\mathcal{B}} = R_I^B \cdot \mathbf{S}_{\mathcal{I}} \tag{3.52}$$

where R_I^B is the DCM from the inertial to body frame.

Sensor Layout and Response The CubeSat is equipped with six coarse sun sensors, one on each face, aligned along the $\pm X$, $\pm Y$, and $\pm Z$ body axes (see Figure 3.11). Each sensor has a cosine response:

$$z_i = \max\left(0, \hat{\mathbf{n}}_i^\top \mathbf{S}_{\mathcal{B}}\right), \quad i = 1, \ldots, 6 \tag{3.53}$$

where $\hat{\mathbf{n}}_i$ is the normal vector of the i-th sensor surface.

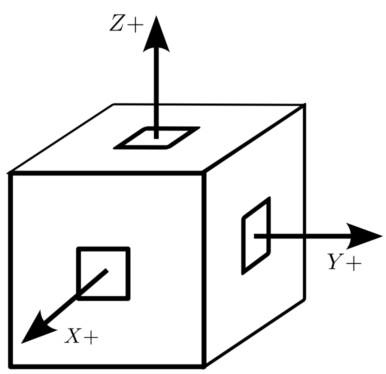

Figure 3.9: Orientation of the six coarse sun sensors on the CubeSat

Measurement Noise Each CSS reading is perturbed with zero-mean Gaussian noise. The noise standard deviation σ is specified in degrees and converted to radians:

$$\mathbf{z}_{\mathrm{CSS}} = \max\left(0, \mathbf{z}_{\mathrm{CSS}} + \mathcal{N}(0, \sigma^2)\right), \quad \sigma = \deg 2rad(\mathrm{CSS}_{\mathrm{noise}}) \tag{3.54}$$

Negative readings are clamped to zero since physical sensors cannot detect negative intensity.

Sun Vector Estimation The estimated Sun vector in the body frame is reconstructed using a weighted sum of the face normals:

$$\hat{\mathbf{S}}_{\mathcal{B}} = \sum_{i=1}^{6} z_i \cdot \hat{\mathbf{n}}_i \tag{3.55}$$

The result is normalized to produce a unit vector:

$$\hat{\mathbf{S}}_{\mathcal{B}} = \frac{\hat{\mathbf{S}}_{\mathcal{B}}}{|\hat{\mathbf{S}}_{\mathcal{B}}|} \tag{3.56}$$

Add some results

3.4.5 Magnetometer

The magnetometer measurement is modeled as a unit vector pointing along the direction of the Earth's magnetic field as observed from the satellite body frame. To approximate this field, a simplified model is used in which the magnetic field points toward the geographic North Pole and is tangential to the Earth's surface at the satellit's location, with an optional dip angle to simulate inclination.

Step 1: Earth-Fixed Transformation

To determine the orientation of the magnetic field relative to the Earth-fixed frame, the satellite position vector $\mathbf{r}_{\mathcal{I}}$ in the inertial (ECI) frame is first transformed to the Earth-fixed (ECEF) frame using a rotation matrix that accounts for Earth's rotation angle at time t:

$$\mathbf{r}_{\mathcal{R}} = R_{\mathcal{I}}^{\mathcal{R}}(t) \cdot \mathbf{r}_{\mathcal{I}} \tag{3.57}$$

where $R_{\mathcal{I}}^{\mathcal{R}}(t)$ is a time-dependent rotation matrix based on the Earth rotation rate ω_e.

Step 2: Direction to Magnetic North

The geographic North Pole is approximated by a fixed point on the Z-axis of the Earth-fixed frame:

$$\mathbf{p}_{NP,\mathcal{R}} = \begin{bmatrix} 0 \\ 0 \\ R_E \end{bmatrix} \tag{3.58}$$

The direction vector from the satellite to the North Pole is then computed as:

$$\mathbf{d}_{NP} = \mathbf{p}_{NP,\mathcal{R}} - \mathbf{r}_{\mathcal{R}} \tag{3.59}$$

Step 3: Tangential Magnetic Field Model

The local radial unit vector from the Earth's center is:

$$\mathbf{u}_{r,\mathcal{R}} = \frac{\mathbf{r}_{\mathcal{R}}}{|\mathbf{r}_{\mathcal{R}}|} \tag{3.60}$$

To simulate a magnetic field that is tangential to Earth's surface, the component of $\mathbf{d}_{NP}$ in the radial direction is removed:

$$\mathbf{z}_{\text{Mag},\mathcal{R}} = \mathbf{d}_{NP} - (\mathbf{d}_{NP} \cdot \mathbf{u}_{r,\mathcal{R}})\mathbf{u}_{r,\mathcal{R}} \tag{3.61}$$

This tangential field vector is then normalized:

$$\mathbf{z}_{\text{Mag},\mathcal{R}} = \frac{\mathbf{z}_{\text{Mag},\mathcal{R}}}{|\mathbf{z}_{\text{Mag},\mathcal{R}}|} \tag{3.62}$$

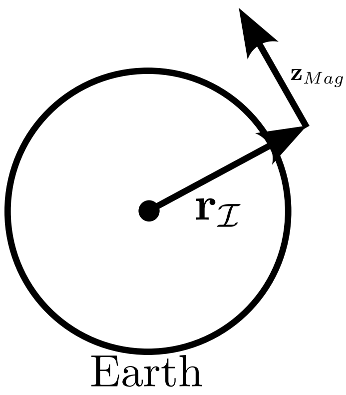

Figure 3.10

Step 4: Dip Angle Adjustment

To simulate magnetic inclination, a rotation about the local East direction is applied to tilt the magnetic field by a dip angle δ, which is measured downward from the local horizontal plane:

$$\mathbf{z}_{\mathrm{Mag},\mathcal{R}}^{\mathrm{incl}} = \cos(\delta)\,\mathbf{z}_{\mathrm{Mag},\mathcal{R}} + \sin(\delta)\,(\mathbf{e}_{\mathrm{East}} \times \mathbf{z}_{\mathrm{Mag},\mathcal{R}}) \tag{3.63}$$

Here, $\mathbf{e}_{\mathrm{East}}$ is the local east direction, obtained via:

$$\mathbf{e}_{\mathrm{East}} = \frac{\mathbf{u}_{r,\mathcal{R}} \times \mathbf{z}_{\mathrm{Mag},\mathcal{R}}}{|\mathbf{u}_{r,\mathcal{R}} \times \mathbf{z}_{\mathrm{Mag},\mathcal{R}}|} \tag{3.64}$$

Step 5: Reference Frame Transformations

The inclined magnetic field vector is transformed back to the inertial frame using:

$$\mathbf{z}_{\mathrm{Mag},\mathcal{I}} = R_{\mathcal{R}}^{\mathcal{I}}(t) \cdot \mathbf{z}_{\mathrm{Mag},\mathcal{R}}^{\mathrm{incl}} \tag{3.65}$$

The final transformation to the spacecraft body frame is performed using the spacecraft attitude quaternion $\mathbf{q}_{\mathcal{B}}^{\mathcal{I}}$, resulting in:

$$\mathbf{z}_{\mathrm{Mag},\mathcal{B}} = R(\mathbf{q}_{\mathcal{B}}^{\mathcal{I}}) \cdot \mathbf{z}_{\mathrm{Mag},\mathcal{I}} \tag{3.66}$$

where $R(\mathbf{q})$ is the direction cosine matrix corresponding to the quaternion $\mathbf{q}$.

Step 6: Measurement Noise

To simulate realistic sensor output, a small-angle random rotation is applied to the vector $\mathbf{z}_{\mathrm{Mag},\mathcal{B}}$ to represent magnetometer noise. This is modeled by sampling a noise rotation axis and applying a perturbation angle drawn from a Gaussian distribution with a standard deviation σ_{noise} (in radians). The rotation is implemented via a noise quaternion and applied to the magnetic field vector.

Step 7: Output

The final estimated magnetometer vector $\hat{\mathbf{z}}_{\mathrm{Mag},\mathcal{B}}$ is normalized and output for use in state estimation:

$$\hat{\mathbf{z}}_{\mathrm{Mag},\mathcal{B}} = \frac{\mathbf{z}_{\mathrm{Mag},\mathcal{B}}}{|\mathbf{z}_{\mathrm{Mag},\mathcal{B}}|} \tag{3.67}$$

This provides a realistic simulation of a three-axis magnetometer, with both geographic dependence and sensor-level noise, for use in spacecraft attitude determination or estimation filters.

3.4.6 TRIAD Attitude Estimation

The TRIAD (Tri-Axial Attitude Determination) algorithm is a deterministic method used to estimate a spacecraft's attitude from two independent, non-collinear direction measurements expressed in both the body and inertial frames. In this work, the TRIAD method is applied using sun vector measurements from a coarse sun sensor and magnetic field measurements from a three-axis magnetometer.

Step 1: Sensor Measurements in Body Frame

Let $\mathbf{s}_\mathcal{B}$ denote the unit vector pointing toward the Sun in the body frame, and $\mathbf{m}_\mathcal{B}$ the unit magnetic field vector in the body frame. These vectors are obtained from sensor measurements and normalized:

$$\mathbf{s}_\mathcal{B} = \frac{\mathbf{s}_\mathcal{B}}{|\mathbf{s}_\mathcal{B}|}, \quad \mathbf{m}_\mathcal{B} = \frac{\mathbf{m}_\mathcal{B}}{|\mathbf{m}_\mathcal{B}|} \tag{3.68}$$

Step 2: Reference Vectors in Inertial Frame

The inertial-frame counterparts to the measured vectors are defined as follows:

- The Sun vector in the inertial (ECI) frame is approximated by the unit vector:

$$\mathbf{s}_\mathcal{I} = \begin{bmatrix} 1 \\ 0 \\ 0 \end{bmatrix} \tag{3.69}$$

- The magnetic field vector in the inertial frame, $\mathbf{m}_\mathcal{I}$, is computed based on the spacecraft position $\mathbf{r}_\mathcal{I}$, a user-defined magnetic dip angle, and Earth's rotation:

$$\mathbf{m}_\mathcal{I} = \text{MagnetometerModel}(\mathbf{r}_\mathcal{I}, t, \omega_e, \delta) \tag{3.70}$$

Both reference vectors are normalized:

$$\mathbf{s}_\mathcal{I} = \frac{\mathbf{s}_\mathcal{I}}{|\mathbf{s}_\mathcal{I}|}, \quad \mathbf{m}_\mathcal{I} = \frac{\mathbf{m}_\mathcal{I}}{|\mathbf{m}_\mathcal{I}|} \tag{3.71}$$

Step 3: Constructing Orthogonal Triads

Two orthonormal vector triads are constructed from the body and reference measurements.

- In the inertial frame:

$$\mathbf{v}_1^\mathcal{I} = \mathbf{s}_\mathcal{I} \tag{3.72}$$

$$\mathbf{v}_2^\mathcal{I} = \frac{\mathbf{s}_\mathcal{I} \times \mathbf{m}_\mathcal{I}}{|\mathbf{s}_\mathcal{I} \times \mathbf{m}_\mathcal{I}|} \tag{3.73}$$

$$\mathbf{v}_3^\mathcal{I} = \mathbf{v}_1^\mathcal{I} \times \mathbf{v}_2^\mathcal{I} \tag{3.74}$$

- In the body frame:

$$\mathbf{v}_1^\mathcal{B} = \mathbf{s}_\mathcal{B} \tag{3.75}$$

$$\mathbf{v}_2^\mathcal{B} = \frac{\mathbf{s}_\mathcal{B} \times \mathbf{m}_\mathcal{B}}{|\mathbf{s}_\mathcal{B} \times \mathbf{m}_\mathcal{B}|} \tag{3.76}$$

$$\mathbf{v}_3^\mathcal{B} = \mathbf{v}_1^\mathcal{B} \times \mathbf{v}_2^\mathcal{B} \tag{3.77}$$

These vectors form right-handed orthonormal bases (triads) in their respective frames.

Step 4: Attitude Rotation Matrix

The attitude rotation matrix $R_{\mathcal{I}}^{\mathcal{B}}$, which rotates vectors from the inertial frame to the body frame, is computed by aligning the inertial and body triads:

$$T_{\mathcal{I}} = \begin{bmatrix} \mathbf{v}_1^{\mathcal{I}} & \mathbf{v}_2^{\mathcal{I}} & \mathbf{v}_3^{\mathcal{I}} \end{bmatrix}, \quad T_{\mathcal{B}} = \begin{bmatrix} \mathbf{v}_1^{\mathcal{B}} & \mathbf{v}_2^{\mathcal{B}} & \mathbf{v}_3^{\mathcal{B}} \end{bmatrix} \tag{3.78}$$

$$R_{\mathcal{I}}^{\mathcal{B}} = T_{\mathcal{B}} \cdot T_{\mathcal{I}}^{\top} \tag{3.79}$$

Step 5: Quaternion Conversion

The attitude quaternion $\mathbf{q}_{\mathcal{B}}^{\mathcal{I}}$ corresponding to the rotation matrix $R_{\mathcal{I}}^{\mathcal{B}}$ is computed using a standard matrix-to-quaternion conversion:

$$\mathbf{q}_{\mathcal{B}}^{\mathcal{I}} = \mathrm{rotm2quat}(R_{\mathcal{I}}^{\mathcal{B}}) \tag{3.80}$$

This quaternion is expressed in scalar-first format:

$$\mathbf{q}_{\mathcal{B}}^{\mathcal{I}} = \begin{bmatrix} q_s & q_x & q_y & q_z \end{bmatrix}^{\top} \tag{3.81}$$

The TRIAD method thus yields a closed-form attitude estimate without optimization or iteration. While it is highly efficient, its accuracy depends on the orthogonality and noise properties of the sensor measurements.

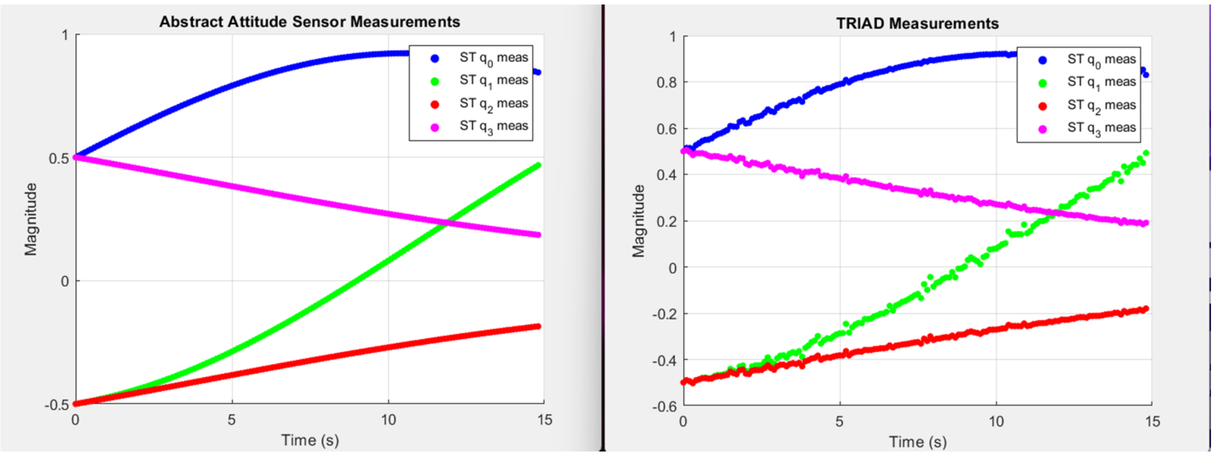

Figure 3.11

3.4.7 Sensors Comparison

Table 3.1: Your table caption

	Noise Profile	Drift Rate	Sampling Rate [Hz]
GPS	10 m	3 m	10
Gyroscope	0.05 deg	1e-3 deg	50
Star Tracker	0.002 deg	-	1
CSS	5 deg	-	2
Magnetometer	10 deg	-	2

3.5 Conclusion

Chapter 4

Image Processing

4.1 Introduction

4.2 Pinhole Camera Model

The ideal pinhole camera can be described as a plane and an optical center (a.k.a) the pinhole. Light will travel from an object throught the optical center. And hit the plane at the opposite end of the optical center. The distance between the opitical center and the plane is called the focal length f.

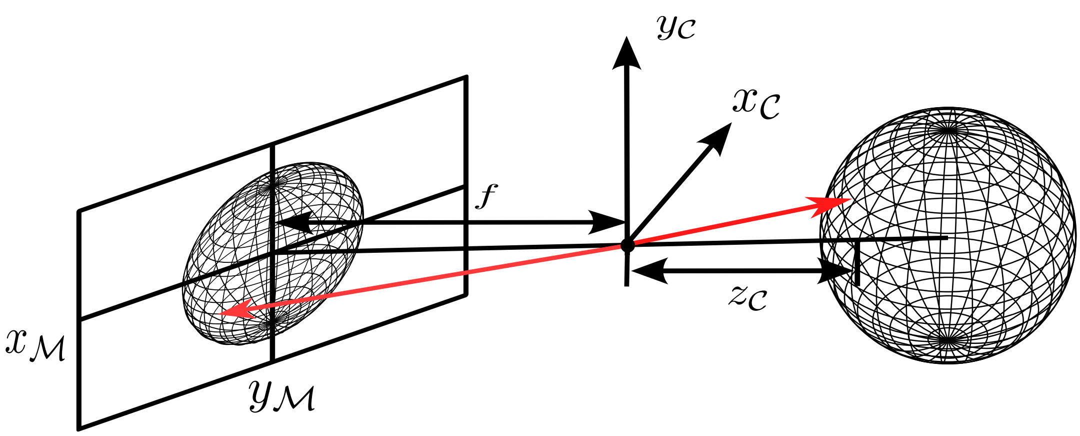

Figure 4.1: PinHole Model

The equation for the pinhole camera model is the following.

$$\begin{bmatrix} x_{\mathcal{M}} \\ y_{\mathcal{M}} \\ 1 \end{bmatrix} = \frac{-f}{z_{\mathcal{C}}} \begin{bmatrix} x_{\mathcal{C}} \\ y_{\mathcal{C}} \\ z_{\mathcal{C}} \end{bmatrix} \tag{4.1}$$

As we can see in the figure this also causes the image tp flip.

Also images are measured with the x-axis going from right to left and the y-axis going from top to bottom so one more transformation needs to be done.

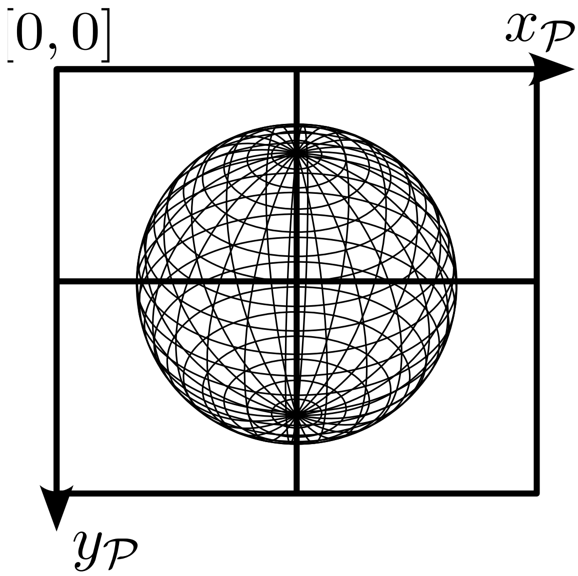

Figure 4.2: Image Plane

$$\begin{bmatrix} x_{\mathcal{P}} \\ y_{\mathcal{P}} \end{bmatrix} = \begin{bmatrix} -x_{\mathcal{M}} + \frac{\text{ImgWidth}}{2} \\ y_{\mathcal{M}} + \frac{\text{ImgHeight}}{2} \end{bmatrix} \tag{4.2}$$

4.2.1 Camera Reference Frame

The camera refrence frame denoted by $\mathcal{C}$. In many Earth Observation missions the camera has its own reference frame defined relative to the Earth. Where the x-axis is pointing directly to the Earth's surface indicatting the cameras roll axis, with the y-axis representing the pitch axis represents an angle ahead or behind of the orbit and the z-axis representing the yaw axis.

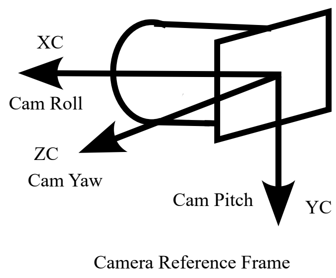

Figure 4.3

$$\mathbf{f}_{\mathcal{C}} = \mathbf{A}_{\mathcal{O}}^{\mathcal{C}} \times \mathbf{f}_{\mathcal{O}} \tag{4.3}$$

4.2.2 Image Reference Frame

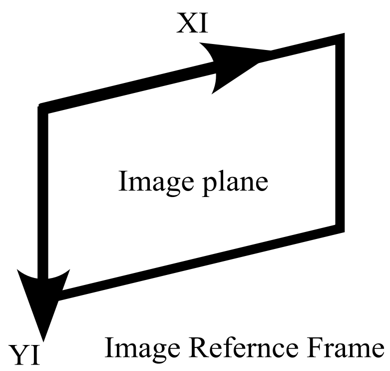

Figure 4.4

4.2.3 Intrinsic Camera Parameters

The projection plane coordinates of the projected point P can be converted into pixel baed measurements by expanding the projection matrix.

A horizontal and verticle scale factor s_u and s_v are defined as

$$s_u = \frac{\text{horizontal image resolution}}{\text{horizontal sensor size}} \tag{4.4}$$

$$s_v = \frac{\text{vertical image resolution}}{\text{vertical sensor size}} \tag{4.5}$$

In the above equations, image resolution refers to the size, in pixels, of the resulting image captures by the modelled camera. Sensor size refers to the physical size of the sensor, this means the scaling factor can be seen as having a unit of pixels per distance. These scaling factors can be incorporated with the focal length of the camera to create factors f_u and f_v so that

$$f_u = s_u f \tag{4.6}$$

$$f_v = s_v f \tag{4.7}$$

Pixel based coordinates of the projected point $\mathbf{p}$ can be calculated with

$$s \begin{bmatrix} u \\ v \\ 1 \end{bmatrix} = \begin{bmatrix} f_u & 0 & 0 \\ 0 & f_v & 0 \\ 0 & 0 & 1 \end{bmatrix} \begin{bmatrix} p_x \\ p_y \\ p_z \end{bmatrix} \tag{4.8}$$

Where the s is the scaling factor. The Projection matrix in Equation ... can lastly be expanded with the offsets o_u amd o_v that ensure that the pixel-based projection plane coordinates are in the lower-right quadrant, as in the convention with digital image. These offsets are defined as

$$o_u = \frac{\text{horizontal image resolution}}{2} \tag{4.9}$$

$$o_v = \frac{\text{vertical image resolution}}{2} \tag{4.10}$$

Pixel-based coordinated off the projected point $\mathbf{p}$ can be calculated in the typical convention with

$$s \begin{bmatrix} u \\ v \\ 1 \end{bmatrix} = \begin{bmatrix} f_u & \alpha & o_u 0 & f_v & o_v 0 & 0 & 1 \end{bmatrix} \begin{bmatrix} p_x \\ p_y \\ p_z \end{bmatrix} \tag{4.11}$$

$$= \mathbf{K} \begin{bmatrix} p_x \\ p_y \\ p_z \end{bmatrix} \tag{4.12}$$

where $\mathbf{K}$ is known as the intrinsic matrix a skewing factor of α is added to adjust for skewing affects of the camera.

4.2.4 Extrensic Camera Parameters

In the equations it is assumed that the point being projected onto the image plane reference is defined in the camera reference frame. This is not always the case and in certain circumstances the points that have to projected will have to be corrected the camera reference frame first.

An extrinsic camera matrix performs this conversion taks, it is made of a DCM $\mathbf{D}$ and translation vector $\mathbf{t}$ so that

$$[\mathbf{D}|\mathbf{t}] = \begin{bmatrix} d_{11} & d_{12} & d_{13} & t_1 \\ d_{21} & d_{22} & d_{23} & t_2 \\ d_{31} & d_{32} & d_{33} & t_3 \end{bmatrix} \tag{4.13}$$

$$s \begin{bmatrix} u \\ v \\ 1 \end{bmatrix} = \mathbf{K}[\mathbf{D}|\mathbf{t}] \begin{bmatrix} p_x \\ p_y \\ p_z \\ 1 \end{bmatrix} \tag{4.14}$$

4.2.5 Back Projection

The intrinsic camera matrix discussed is typicall used to project 3D points in the camera referecne frame down to the 2D image plane reference frame. It can also be used to project 2D coordinates on the image plane reference frame back into 3D space.

Assume the scaling factor s is known or assumed.

The 3D vector can be reconstructed.

$$\mathbf{d} = s * \mathbf{K}^{-1} \begin{bmatrix} u \\ v \\ 1 \end{bmatrix} \tag{4.15}$$

4.3 Satellite Image Characteristics

4.3.1 Ground Sample Distance

Ground Sampling Distance (GSD) is the real-world distance between the centers of two adjacent pixels measured on the ground in an image captured by a remote sensing system or satellite. It represents the spatial resolution of the imaging sensor and determines the level of detail visible in the image — smaller GSD values correspond to higher resolution, allowing finer features on the ground to be distinguished.

Where the mathematical relationship is

$$GSD = \frac{\text{altitude} * \text{pixelsize} * \text{resolution}}{\text{focal length}} \tag{4.16}$$

4.3.2 Imaging Geometry

The field of view (FOV) of the satellite imager is calculated using the relationship between the camera's focal length, sensor dimensions, and pixel size. The vertical field of view is determined by the equation $\text{FOV}_v = 2 \times \arctan\left(\frac{I_y \times p_s}{2f}\right)$, where I_y is the image height in pixels, p_s is the pixel size, and f is the focal length. For the horizontal field of view, the image width I_x is substituted for I_y in the calculation. This angular field of view defines the observable ground area from the satellite's orbital altitude, with the ground sample distance (GSD) providing the metric resolution per pixel according to $\text{GSD} = \frac{p_s \times h}{f}$, where h is the altitude above the target surface. These geometric relationships are fundamental to the measurement model, as they establish the transformation between pixel coordinates in the image plane and the corresponding angular directions in the camera reference frame, enabling precise feature vector calculations for pose estimation.

4.3.3 Lens Distortions

4.4 Feature Detection and Description

4.4.1 Classical Feature Detectors

4.4.1.1 SIFT

Scale-Invariant Feature Transform (SIFT) is a computer vision algorithm designed to detect and describe local features in images that remain stable under various transformations including scaling, rotation, and illumination changes. The algorithm operates in four main stages: scale-space extrema detection using Difference of Gaussians (DoG), keypoint localization through sub-pixel refinement, orientation assignment based on local gradient histograms, and descriptor generation using a 128-dimensional feature vector.

The scale-space representation is constructed by convolving the input image $I(x, y)$ with Gaussian kernels of increasing standard deviation:

$$L(x, y, \sigma) = G(x, y, \sigma) * I(x, y) \tag{4.17}$$

where $G(x, y, \sigma) = \frac{1}{2\pi\sigma^2} e^{-(x^2+y^2)/2\sigma^2}$ is the Gaussian kernel. The DoG function approximates the Laplacian of Gaussian for efficient keypoint detection:

$$D(x, y, \sigma) = L(x, y, k\sigma) - L(x, y, \sigma) \tag{4.18}$$

where k is a constant multiplicative factor between adjacent scales.

For each detected keypoint, the dominant orientation is determined by computing the gradient magnitude and direction:

$$m(x, y) = \sqrt{[L(x+1, y) - L(x-1, y)]^2 + [L(x, y+1) - L(x, y-1)]^2} \tag{4.19}$$

$$\theta(x, y) = \arctan\left(\frac{L(x, y+1) - L(x, y-1)}{L(x+1, y) - L(x-1, y)}\right) \tag{4.20}$$

The descriptor is constructed by sampling gradients in a 16×16 pixel neighborhood around the keypoint, subdivided into 4×4 blocks with 8-bin orientation histograms, resulting in a 128-dimensional feature vector ($4 \times 4 \times 8 = 128$). Each descriptor element is weighted by the gradient magnitude and a Gaussian window centered at the keypoint. The resulting 128-dimensional descriptor provides robust matching capabilities across different viewing conditions, making SIFT particularly suitable for satellite imagery where features must be reliably detected despite changes in lighting, seasonal variations, and slight geometric distortions. However, the computational complexity of SIFT can be limiting for real-time applications, requiring careful consideration of the trade-off between feature quality and processing speed in resource-constrained satellite systems.

4.4.1.2 SURF

Speeded-Up Robust Features (SURF) is a computer vision algorithm developed as a faster alternative to SIFT while maintaining comparable performance in feature detection and description. SURF achieves computational efficiency through the use of integral images and approximations of the Laplacian of Gaussian operator, making it particularly suitable for real-time applications in resource-constrained satellite systems.

The algorithm utilizes integral images $I_\Sigma(x, y)$ to enable rapid computation of rectangular area sums:

$$I_\Sigma(x, y) = \sum_{i=0}^{i \leq x} \sum_{j=0}^{j \leq y} I(i, j) \tag{4.21}$$

where $I(i, j)$ represents the intensity at pixel (i, j). This allows any rectangular sum to be computed in constant time using only four array references.

SURF approximates the Laplacian of Gaussian using box filters that can be evaluated efficiently with integral images. The determinant of the Hessian matrix is used for keypoint detection:

$$\text{Det}(\mathbf{H}) = D_{xx} D_{yy} - (0.9 D_{xy})^2 \tag{4.22}$$

where D_{xx}, D_{yy}, and D_{xy} are the convolution responses of the image with the second-order Gaussian derivatives, approximated using box filters. The factor 0.9 is an empirical weight to balance the expression.

For orientation assignment, SURF computes Haar wavelet responses in the x and y

directions within a circular neighborhood:

$$d_x = \text{Haar}_x * I(x, y) \tag{4.23}$$

$$d_y = \text{Haar}_y * I(x, y) \tag{4.24}$$

The dominant orientation is determined by summing all responses within a sliding window of $\frac{\pi}{3}$ radians.

The SURF descriptor is typically 64-dimensional (compared to SIFT's 128), constructed by dividing a 20×20 pixel region around the keypoint into 4×4 sub-regions. For each sub-region, the wavelet responses are summed to create a 4-dimensional descriptor vector $\mathbf{v} = [\sum d_x, \sum d_y, \sum |d_x|, \sum |d_y|]$. This results in a $4 \times 4 \times 4 = 64$-dimensional descriptor that provides robust matching while requiring significantly less computational resources than SIFT, making it advantageous for satellite pose estimation applications where processing efficiency is critical.

4.4.1.3 ORB

Oriented FAST and Rotated BRIEF (ORB) is a binary feature descriptor that combines the FAST keypoint detector with the BRIEF descriptor, enhanced with orientation compensation to achieve rotation invariance. ORB is designed for real-time applications and provides significant computational advantages over SIFT and SURF, making it particularly suitable for resource-constrained satellite systems where processing efficiency is paramount.

The FAST (Features from Accelerated Segment Test) detector identifies keypoints by examining the intensity values of 16 pixels arranged in a circle around a candidate point p. A pixel p is classified as a corner if there exists a set of n contiguous pixels in the circle that are all brighter than $I_p + t$ or all darker than $I_p - t$, where I_p is the intensity of pixel p and t is a threshold:

$$\text{FAST}(p) = \begin{cases} 1 & \text{if } \exists \text{ arc of length } n \text{ such that } \forall x \in \text{arc} : |I_x - I_p| > t \\ 0 & \text{otherwise} \end{cases} \tag{4.25}$$

To achieve rotation invariance, ORB computes the intensity centroid to determine keypoint orientation. The moments of a patch are calculated as:

$$m_{pq} = \sum_{x,y} x^p y^q I(x, y) \tag{4.26}$$

$$\text{Centroid: } \mathbf{C} = \left(\frac{m_{10}}{m_{00}}, \frac{m_{01}}{m_{00}} \right) \tag{4.27}$$

The orientation angle is then determined by:

$$\theta = \arctan\left(\frac{m_{01}}{m_{10}}\right) \tag{4.28}$$

The BRIEF descriptor is modified to create rBRIEF (rotated BRIEF) by applying a rotation matrix to the sampling pattern. For a set of n binary tests, each test τ compares the intensities of two pixels:

$$\tau(p; x, y) = \begin{cases} 1 & \text{if } p(x) < p(y) \\ 0 & \text{otherwise} \end{cases} \tag{4.29}$$

The rotated sampling pattern is computed as:

$$\mathbf{S}_\theta = \mathbf{R}_\theta \mathbf{S} \tag{4.30}$$

where $\mathbf{R}_\theta$ is the rotation matrix and $\mathbf{S}$ is the original sampling pattern.

The final ORB descriptor is a 256-bit binary string computed by applying the rotated BRIEF tests. This binary representation enables extremely fast matching using the Hamming distance, computed as:

$$d_H(\mathbf{a}, \mathbf{b}) = \sum_{i=1}^{n} a_i \oplus b_i \tag{4.31}$$

where $\oplus$ denotes the XOR operation. The computational efficiency and low memory requirements of ORB make it ideal for satellite pose estimation applications where real-time performance and limited computational resources are critical constraints.

4.4.1.4 Comparison

4.5 Measurement Extraction

4.5.1 Image Generation

4.5.1.1 Rendering the Earth

To create an image

Fisrt a High resolution image is sticth in QGIS, a type fo Geographic information system, used to open an edit geolocated images. Images a downloaded from the copernicus with a GSD of 15 m.

Insert Image of Paris Inert Image of Pyramids Insert Image of Hawaii Volcano

After an high resolution image is sitched. It is rasterised. This rasterised image with all its goelocation data is then projected onto a WGS84 ellipsoid.

Figure 4.5: High Resolution Image projected on Ellipsoid

The Low resolution Earth in the Backgorund is used as a place holder to test results

4.5.2 Earth Tracker Algorithm

The Earth Tracker works on the same principle as Back projection.

Step 1: Translate pixels to optical center

The second step involes translating the pixel cooridnates to the optical center as the origin. This transformation accounts for the camera's principle point offset, where I_x and I_y represent width and height, repsectivly. The resulting coordinate vector $\mathbf{f}_{\mathcal{M}/\mathcal{S}}$ represents position Relative to the camera boresight.

$$\mathbf{f_{M/S}} = \begin{bmatrix} f_{\mathcal{M}} - \frac{I_x}{2} \\ f_{\mathcal{M}} - \frac{I_y}{2} \end{bmatrix} \text{(Pixels)} \tag{4.32}$$

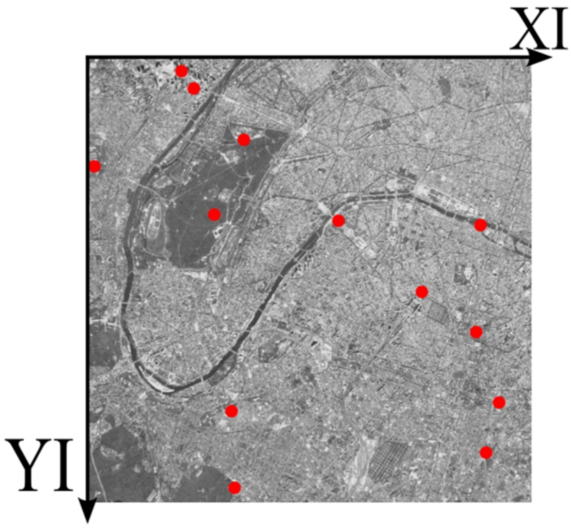

Figure 4.6: Origin Correction

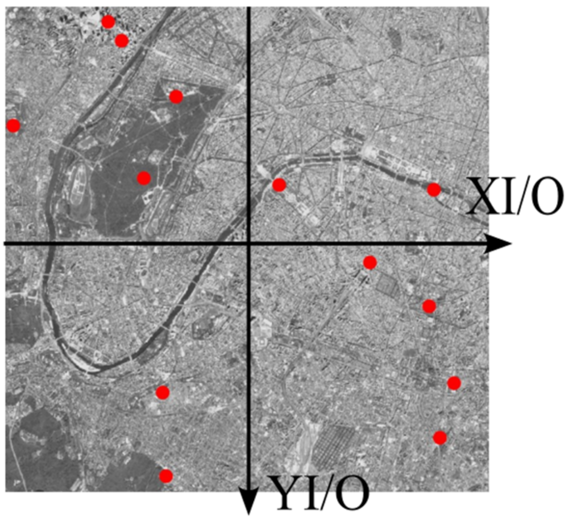

Figure 4.7: Origin Correction 2

Step 2: Three-Dimentional Ray Vector Construction

This step transform the 2 dimensional pixel coordinates into the three-dimensional direction vector in the camera frame. The vector $\mathbf{f}_{\mathcal{M}/\mathcal{F}}$ represents the feqture direction relative to the camera focal point, where the z-component is dtermined by the effective focal lenght in pixels

$$\mathbf{f}_{\mathcal{M}/\mathcal{F}} = \begin{bmatrix} f_{\mathcal{M}/\mathcal{S}_\S} \\ f_{\mathcal{M}/\mathcal{S}_\dagger} \\ \frac{fl}{ps} \end{bmatrix} \tag{4.33}$$

Step 3: Scale dorection vector

The 3rd step performs a cordinate transformation to orient the feature vector in the appropriate referecne direction. This operation inverts and scales the vector so that it is correct in the camera reference frame

The sacling used is the assumed GSD

$$\mathbf{f} = GSD \times \mathbf{f} \tag{4.34}$$

4.5.3 Geolocation Process

For the geolocation.

Step 1: Chip Image

Step 2: Chip features

Step 3: Use SIFT for feauture matching

Step 4: Add geolocation

4.5.4 Practical Considerations

4.5.4.1 Number of Valid Features

4.5.5 Conclusion

Chapter 5

State Estimation

5.1 Introduction

5.2 Recursive Estimation

This section describes the element of recrusive estimators along with a few commonly-used estimators in the fields of localisation and tracking. A recursive estimoter uses the previous distrubution over a set of systm states and curent sensor data to estimte the current state distribution. Figure 3.1 illustrates the basic workings of a discrete recursive filter.

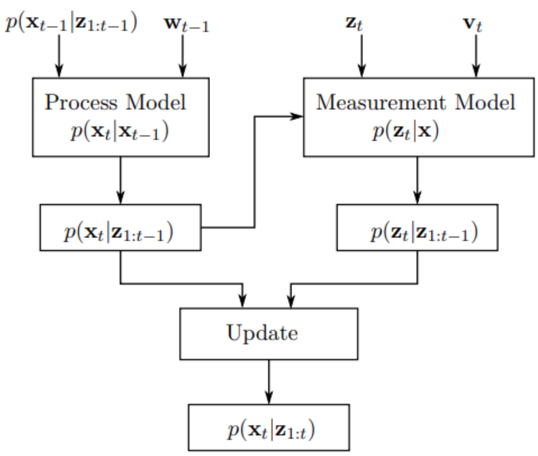

Figure 5.1: Recursive estimator algorithm flowchart

The state vector is represented by $\mathbf{x}_t$ for the estimation problem in the discrete time domain. The process, or the state transition function, is expressed As

$$\mathbf{x}_t = \mathbf{f}(\mathbf{x}_{t-1}, \mathbf{u}_{t-1}, \mathbf{w}_{t-1}) \tag{5.1}$$

where $\mathbf{f}$ is either a linear or non-linear transtion fucntion and $\mathbf{w}_t$ represents the process noise. New observation data, $\mathbf{z}_t$, is available at discrete timesteps and can be related to $\mathbf{x}_t$ by the measurement function,

$$\mathbf{z}_t = \mathbf{h}(\mathbf{x}_t, \mathbf{v}_t) \tag{5.2}$$

The measurement uncertainty is represented by $\mathbf{v}_t$ and $\mathbf{h}$ is the observation model, which can also either be linear or non-linear. The goal is to obtain the posterior distribution, $p(\mathbf{x}|\mathbf{z}_{1:t})$, over the state vector $\mathbf{x}_t$. This is done by recursively performing the process and measurement updates.

At a time t, the posterior distribution over $\mathbf{x}_{t-1}$ at time $t-1$ is known and the prior distribution at t is calcualted As

$$p(\mathbf{x}_t|\mathbf{z}_{1:t-1}) = \int p(\mathbf{x}_t|\mathbf{x}_{t-1})p(\mathbf{x}_{t-1}|\mathbf{z}_{1:t-1})\ d\mathbf{x}_{t-1} \tag{5.3}$$

The measruement update is used to calculate the new posterior, at time t , given the prior state distribution according to Bayes' rule,

$$p(\mathbf{x}_t|\mathbf{z}_{1:t}) = \frac{p(\mathbf{z}_t|\mathbf{x}_t)p(\mathbf{x}_t|\mathbf{z}_{1:t-1})}{p(\mathbf{z}_t|\mathbf{z}_{1:t-1})} \tag{5.4}$$

The Kalman filter is a popular estimator used in pose estimation porblems. It is a special case of the Bayes filter, where the Guassian noise distributions are assumed. The assumption is also made that the initial distibution of the system can be represented by a Gaussian distribution. A control and measurement update is executed at each sampling instant to update the distibutionover the states. If the previous state distribution is Gaussian, then the updated current distribution will also be Gaussian and therefore the best estimate is chosen as the mean of the distribution.

Differen variants of the Kalman Filter exists, of which the extended and unscented Kalman Filter are the most popular, eah with their own unique characteristics.

The extended Kalman Filter (EKF) overcomes the restrictions of the linear filter by approximating non-linear functions to be linear using a first-order Taylor expansion. The mean position of the state vector is used as the linearisation point around which the tangent of the non-linear function is calcualted, allowing the use of standard Kalman Filter equations. It is typically more efficient than other non-linear filters which sometimes comes at a cost or reduced accuracy.

The unscented Kalman Filter (UKF) uses stochiatic linearisation to deal with non-linear systems. Given a distribution with a known mean and covariance, a set of weighted points, known as sigma points, are chosen and transformed using the non-linear function. A new distribution is determined from the transformed sigma points. The process and observation functions do not need to be differentiable and the output is based on vlaues in a larger region, rather than a local approximation.

5.3 Kalman Filter

Kalman filters are well suited for localistation problems since the nature of these systems are normally non-linear. Both the linear and non-linear variants of the Kalman Filter are concenerd with estimating states using motion model to perform this data fusion. The following equations are used to model the system.

$$\mathbf{x}_t = A_t\mathbf{x}_{t-1} + B\mathbf{u}_{t-1} + \epsilon\mathbf{z}_t = C_t\mathbf{x}_t + \zeta \tag{5.5}$$

where

$$\epsilon = \mathcal{N}(\mathbf{0}; R)\zeta = \mathcal{N}(\mathbf{0}; Q) \tag{5.6}$$

The matrices R and Q are the known covarianve matrices of the process and observation noise, repsectivly and the matrices A, B and C form part of the linear functions.

These equations can be used to calculate the posterior distrobution

$$p(\mathbf{y}_t|\mathbf{u}_{1:t}, \mathbf{z}_{1:t}) = \mathcal{N}(\mu_t; \Sigma_t) \tag{5.7}$$

The state estimation problem in this project makes use of non-linear system models, and a high-dimensinal state space. The EKF is well suited for this problem, since it accomodates non-linear process and observation models and is capable of dealing with high-dimensional state spaces. The EKF os often use for the SLAM problem and is well known in the field of robotics and localisation.

The rigid body motion models and measurements models of systems are, however, non-linear. Therefore, a general non-linear description is used for the motion and measurement models

$$\mathbf{y}_t = \mathbf{g}(\mathbf{y}_{t-1}, \mathbf{u}_t) + \boldsymbol{\epsilon} \tag{5.8}$$

$$\mathbf{z}_t = \mathbf{h}(\mathbf{y}_t) + \boldsymbol{\zeta} \tag{5.9}$$

The motion and measurement functions, $\mathbf{g}$ and $\mathbf{h}$, are non-linear vector functions. These are linearised to enable the use of the Kalman filter equations. The non-linear vector functions, $\mathbf{f}(\mathbf{x}) = [f_1(\mathbf{x}), f_2(\mathbf{x}), ..., f_m(\mathbf{x})]^T$, is linearised around its mean value, μ, using a Taylor series expansion.

$$\mathbf{f}(\mathbf{x}) \approx \mathbf{f}(\boldsymbol{\mu}) + \mathbf{f}'(\boldsymbol{\mu})(\mathbf{x} - \boldsymbol{\mu}) \tag{5.10}$$

where

$$
\begin{aligned}
\mathbf{f}'(\mathbf{x}) = F(\mathbf{x}) &= \frac{\partial \mathbf{f}(\mathbf{x})}{\partial \mathbf{x}} \\
&= \begin{bmatrix} \frac{\partial f_1}{\partial x_1} & \cdots & \frac{\partial f_1}{\partial x_n} \\ \vdots & \ddots & \vdots \\ \frac{\partial f_m}{\partial x_1} & \cdots & \frac{\partial f_m}{\partial x_n} \end{bmatrix}_{m \times n}
\end{aligned} \tag{5.11}
$$

$F(\mathbf{x})$ is referred to as the Jacobian matrix. Using this linearisation, the vector function, $\mathbf{g}$ and $\mathbf{h}$ are approximated as,

$$\mathbf{y}_{t-1}, \mathbf{u}_t \approx \mathbf{g}(\boldsymbol{\mu}_{t-1}, \mathbf{u}_t) + \mathbf{G}_t(\mathbf{y}_{t-1} - \boldsymbol{\mu}_{t-1}) \tag{5.12}$$

$$\mathbf{h}(\mathbf{y}_t) \approx \mathbf{h}(\boldsymbol{\mu}_t) + \mathbf{H}_t(\mathbf{y}_t - \boldsymbol{\mu}_t) \tag{5.13}$$

where $\mathbf{G}_t$ and $\mathbf{H}_t$ are the Jacobian matrices of $\mathbf{g}$ and $\mathbf{h}$, respectively. This linearisation leads to the approximate distribution

$$p(\mathbf{y}_t \mid \mathbf{u}_{1:t}, \mathbf{z}_{1:t}) \approx \mathcal{N}(\boldsymbol{\mu}_{t|t}, \boldsymbol{\Sigma}_{t|t}) \tag{5.14}$$

5.4 System Modelling

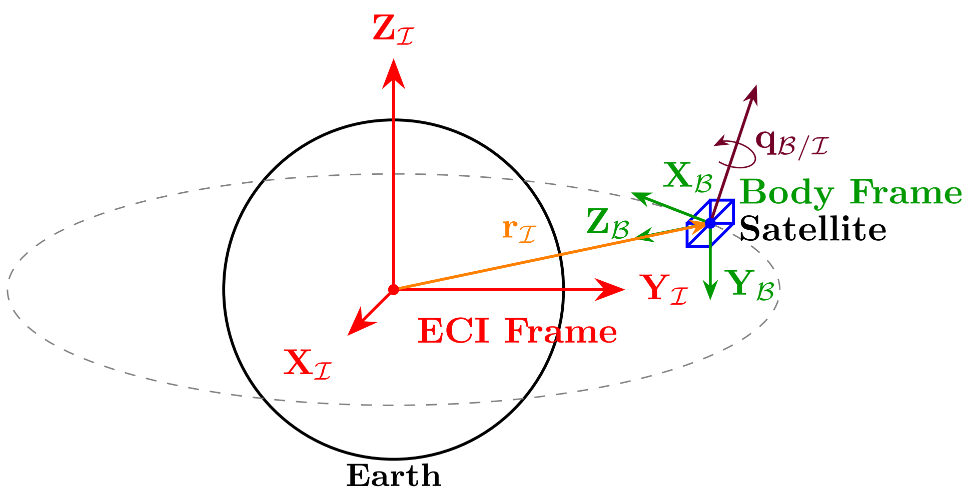

Figure 5.2: Satellite pose estimation concept showing orbital geometry, reference frames

As we can see in Figure 5.2 to determine the pose of the satellite the position and the attitude of the satellite in the ECI reference frames needs to be determines

$$\mathbf{x}_t = \begin{bmatrix} \mathbf{r}_{\mathcal{I}} & \mathbf{v}_{\mathcal{I}} & \mathbf{q}_{\mathcal{B}/\mathcal{I}} & \boldsymbol{\omega}^{\mathcal{B}}_{\mathcal{B}/\mathcal{I}} \end{bmatrix}^T \tag{5.15}$$

5.4.1 Motion Model

The rotation of the satellite body is non-linear and the satellite motion from one timestep to the next when using Newton-Eular coupling can be described by the vector function $\mathbf{g}$,

$$\mathbf{x}_t = \mathbf{g}(\mathbf{x}_{t-1}, \mathbf{u}_t) + \boldsymbol{\epsilon} \tag{5.16}$$

which is expanded to,

$$\mathbf{x}_t = \begin{bmatrix} r_{x,t} \\ r_{y,t} \\ r_{z,t} \\ v_{x,t} \\ v_{y,t} \\ v_{z,t} \\ q_{s,t} \\ q_{x,t} \\ q_{y,t} \\ q_{z,t} \\ \omega_{x,t} \\ \omega_{y,t} \\ \omega_{z,t} \end{bmatrix} = \mathbf{x}_{t-1} + \begin{bmatrix} v_{x,t-1} \\ v_{x,t-1} \\ v_{x,t-1} \\ -\frac{\mu}{|\mathbf{r}|^3} * r_{x,t-1} + J2_{x,t-1} \\ -\frac{\mu}{|\mathbf{r}|^3} * r_{y,t-1} + J2_{y,t-1} \\ -\frac{\mu}{|\mathbf{r}|^3} * r_{z,t-1} + J2_{z,t-1} \\ \frac{1}{2}(-\omega_{x,t-1}q_{x,t-1} - \omega_{y,t-1}q_{y,t-1} - \omega_{z,t-1}q_{z,t-1}) \\ \frac{1}{2}(\omega_{x,t-1}q_{s,t-1} + \omega_{z,t-1}q_{y,t-1} - \omega_{y,t-1}q_{z,t-1}) \\ \frac{1}{2}(\omega_{y,t-1}q_{s,t-1} - \omega_{z,t-1}q_{x,t-1} + \omega_{x,t-1}q_{z,t-1}) \\ \frac{1}{2}(\omega_{z,t-1}q_{s,t-1} + \omega_{y,t-1}q_{x,t-1} - \omega_{x,t-1}q_{y,t-1}) \\ \frac{1}{I_{xx}}(I_{yy} - I_{zz})\omega_{y,t-1}\omega_{z,t-1} \\ \frac{1}{I_{yy}}(I_{zz} - I_{xx})\omega_{z,t-1}\omega_{x,t-1} \\ \frac{1}{I_{zz}}(I_{xx} - I_{yy})\omega_{x,t-1}\omega_{y,t-1} \end{bmatrix} \Delta t + \begin{bmatrix} 0 \\ 0 \\ 0 \\ 0 \\ 0 \\ 0 \\ 0 \\ 0 \\ 0 \\ 0 \\ T_x/I_x \\ T_y/I_y \\ T_z/I_z \end{bmatrix} \tag{5.17}$$

The body-fixed axes of the target are chosen to coincide with its principle axes of inertia. The principle moment of inertia are given barycenter

$$\mathbf{I}_{\mathcal{B}} = \begin{bmatrix} I_{xx} & 0 & 0 \\ 0 & I_{yy} & 0 \\ 0 & 0 & I_{zz} \end{bmatrix} \tag{5.18}$$

External torques, T_x, T_y and T_z, are asssumed to be zero and there is thus no control input, $\mathbf{u}_t$.

Thus

$$\mathbf{x}_t = \mathbf{g}(\mathbf{x}_{t-1}) \tag{5.19}$$

where

$$\mathbf{x}_t = \begin{bmatrix} r_{x,t} \\ r_{y,t} \\ r_{z,t} \\ v_{x,t} \\ v_{y,t} \\ v_{z,t} \\ q_{s,t} \\ q_{x,t} \\ q_{y,t} \\ q_{z,t} \\ \omega_{x,t} \\ \omega_{y,t} \\ \omega_{z,t} \end{bmatrix} = \mathbf{x}_{t-1} + \begin{bmatrix} v_{x,t-1} \\ v_{x,t-1} \\ v_{x,t-1} \\ -\frac{\mu}{|\mathbf{r}|^3} * r_{x,t-1} + J2_{x,t-1} \\ -\frac{\mu}{|\mathbf{r}|^3} * r_{y,t-1} + J2_{y,t-1} \\ -\frac{\mu}{|\mathbf{r}|^3} * r_{z,t-1} + J2_{z,t-1} \\ \frac{1}{2}(-\omega_{x,t-1}q_{x,t-1} - \omega_{y,t-1}q_{y,t-1} - \omega_{z,t-1}q_{z,t-1}) \\ \frac{1}{2}(\omega_{x,t-1}q_{s,t-1} + \omega_{z,t-1}q_{y,t-1} - \omega_{y,t-1}q_{z,t-1}) \\ \frac{1}{2}(\omega_{y,t-1}q_{s,t-1} - \omega_{z,t-1}q_{x,t-1} + \omega_{x,t-1}q_{z,t-1}) \\ \frac{1}{2}(\omega_{z,t-1}q_{s,t-1} + \omega_{y,t-1}q_{x,t-1} - \omega_{x,t-1}q_{y,t-1}) \\ \frac{1}{I_{xx}}(I_{yy} - I_{zz})\omega_{y,t-1}\omega_{z,t-1} \\ \frac{1}{I_{yy}}(I_{zz} - I_{xx})\omega_{z,t-1}\omega_{x,t-1} \\ \frac{1}{I_{zz}}(I_{xx} - I_{yy})\omega_{x,t-1}\omega_{y,t-1} \end{bmatrix} \Delta t \tag{5.20}$$

5.4.2 Measurement Model

5.4.3 Earth Tracker Measurement Model

The Earth Tracker sends 2 inputs to the EKF, the measurement of the Earth tracker itself

$$\mathbf{z}_{ET} = \mathbf{f}_{\mathcal{B}} = \begin{bmatrix} x_{\mathcal{B}} \\ y_{\mathcal{B}} \\ z_{\mathcal{B}} \end{bmatrix} \tag{5.21}$$

And the Geolocated feature vector through feature mathcing also refered to as the catalogue vector. $\mathbf{f}_{\mathcal{R}}$

To transform this vector into a vector to be comparable to the measurement.

$$\mathbf{f}_{\mathcal{B}} = \mathbf{A}^{\mathcal{B}}_{\mathcal{I},t} \times \mathbf{A}^{\mathcal{I}}_{\mathcal{R},t} \times \mathbf{f}_{\mathcal{R}} \tag{5.22}$$

Where $\mathbf{A}^{\mathcal{B}}_{\mathcal{O},t}$ is a function of the the quaternion $\mathbf{q}_{\mathcal{B}/\mathcal{I}}$

5.4.4 Other Sensor Measruement Models

GPS

For the GPS it measures position in the ECEF reference frame, so it need to be converted to toe ECI reference frame.

$$\mathbf{H}_{GPS} = \begin{bmatrix} \cos(\omega_e t) & -\sin(\omega_e t) & 0 & \mathbf{0}_{1\times10} \\ \sin(\omega_e t) & \cos(\omega_e t) & 0 & \mathbf{0}_{1\times10} \\ 0 & 0 & 1 & \mathbf{0}_{1\times10} \end{bmatrix} \tag{5.23}$$

Gyroscope

for the gyroscope, the gyroscope alreadu measures $\boldsymbol{\omega}^{\mathcal{B}}_{\mathcal{B}/\mathcal{I}}$ so it is just a direct relationship.

$$\mathbf{H}_{GYR} = \begin{bmatrix} \mathbf{0}_{1\times10} & 1 & 0 & 0 \\ \mathbf{0}_{1\times10} & 0 & 1 & 0 \\ \mathbf{0}_{1\times10} & 0 & 0 & 1 \end{bmatrix} \tag{5.24}$$

TRIAD and Star Tracker

The Coarse Sun Sensor and Magnetometer measurements are pre-processed into an attitue value of the body frame relative to the Inertial reference frame.$\mathbf{q}_{\mathcal{B}/\mathcal{I}}$

$$\mathbf{H}_{TRIAD} = \begin{bmatrix} \mathbf{0}_{1\times6} & 1 & 0 & 0 & 0 & \mathbf{0}_{1\times3} \\ \mathbf{0}_{1\times6} & 0 & 1 & 0 & 0 & \mathbf{0}_{1\times3} \\ \mathbf{0}_{1\times6} & 0 & 0 & 1 & 0 & \mathbf{0}_{1\times3} \\ \mathbf{0}_{1\times6} & 0 & 0 & 0 & 1 & \mathbf{0}_{1\times3} \end{bmatrix} \tag{5.25}$$

5.5 CONCLUSION

Chapter 6

System Integration

6.1 System Diagram

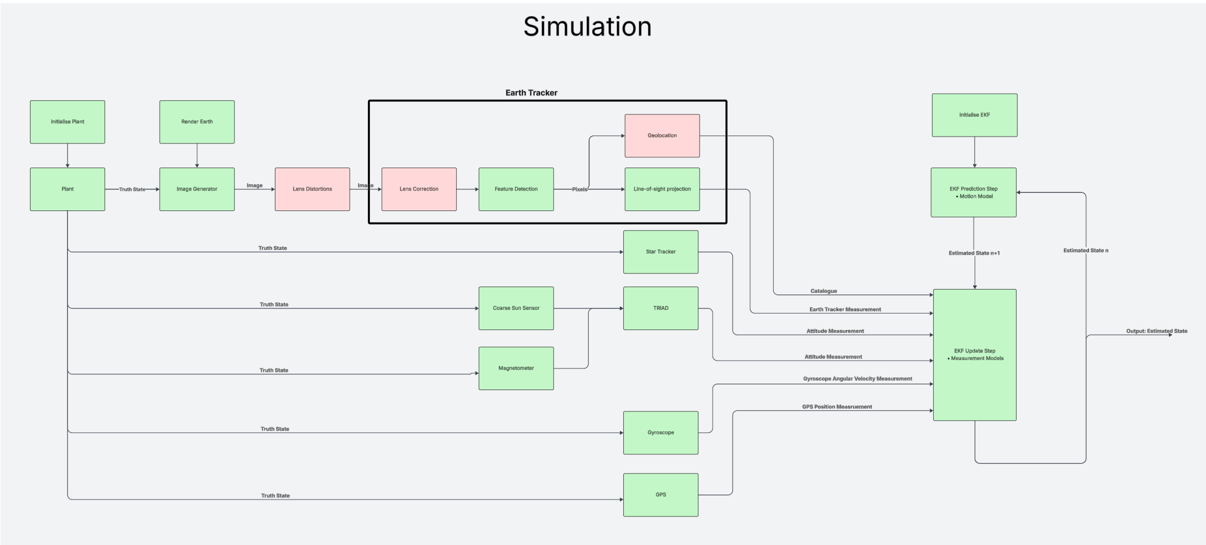

Figure 6.1: Image Plane

6.2 System Initialization

The orbital system is initialized using the following parameters:

- **Latitude**: Initial geodetic latitude of the satellite.
- **Longitude**: Initial geodetic longitude of the satellite.
- **Altitude**: Initial altitude above the WGS84 ellipsoid.

- **Roll (X-axis)**: Initial roll angle of the satellite body with respect to the orbital reference frame.

- **Pitch (Y-axis)**: Initial pitch angle of the satellite body with respect to the orbital reference frame.

- **Yaw (Z-axis)**: Initial yaw angle of the satellite body with respect to the orbital reference frame.

The geodetic latitude, longitude, and altitude are first converted to an inertial position vector using the WGS84 Earth model. This involves a transformation from the local geodetic frame to the Earth-Centered Earth-Fixed (ECEF) frame, followed by a rotation into the inertial frame:

$$\mathbf{r}_{\mathcal{I}} = T_{\mathcal{R}}^{\mathcal{I}} \left(T_{\mathcal{L}}^{\mathcal{R}} (\mathbf{r}_{\mathcal{L}}, \omega_e, t) \right) \tag{6.1}$$

To compute the initial velocity vector, it is assumed that the satellite is in a near-circular orbit, and thus its velocity vector is orthogonal to its position vector. While multiple solutions satisfy this constraint, the velocity direction is resolved using the local east unit vector, which is always tangential to the satellite's position on the Earth's surface. The eastward direction is given by:

$$\mathbf{u}_{\text{east}} = \frac{1}{||\cdot||} \begin{bmatrix} -\sin(\lambda) \\ \cos(\lambda) \\ 0 \end{bmatrix} \tag{6.2}$$

where λ is the geodetic longitude. The vector is normalized to obtain a unit direction. The magnitude of the orbital velocity is computed using the vis-viva equation:

$$||\mathbf{v}|| = \sqrt{\frac{\mu}{||\mathbf{r}||}} \tag{6.3}$$

where μ is the standard gravitational parameter, and $||\mathbf{r}||$ is the norm of the inertial position vector.

The inertial velocity vector is then calculated as:

$$\mathbf{v}_{\mathcal{I}} = ||\mathbf{v}|| \cdot \mathbf{u}_{\text{east}} \tag{6.4}$$

Add some pictures for visualisation

The satellite's initial attitude is defined by two sequential quaternion rotations:

- $q_{\mathcal{O}/\mathcal{I}}$: the quaternion representing the rotation from the inertial (ECI) frame $\mathcal{I}$ to the orbital reference frame $\mathcal{O}$,

* $q_{\mathcal{B}/\mathcal{O}}$: the quaternion representing the rotation from the orbital frame $\mathcal{O}$ to the satellite body frame $\mathcal{B}$,

These quaternions are constructed using the initial orbital position (from latitude, longitude, and altitude) and the initial roll, pitch, and yaw of the satellite body with respect to the orbital frame.

The total attitude of the satellite body with respect to the inertial frame is given by the quaternion composition:

$$q_{\mathcal{B}/\mathcal{I}} = q_{\mathcal{B}/\mathcal{O}} \otimes q_{\mathcal{O}/\mathcal{I}} \tag{6.5}$$

where $\otimes$ denotes quaternion multiplication, performed right-to-left (i.e., the rotation $q_{\mathcal{O}/\mathcal{I}}$ is applied first, followed by $q_{\mathcal{B}/\mathcal{O}}$).

Reference Frame Alignment at Initialization At the simulation start time $t = 0$, it is assumed that the Earth-Centered, Earth-Fixed (ECEF) frame $\mathcal{R}$ is aligned with the inertial frame $\mathcal{I}$. This is a common simplification used in orbital mechanics when time is initialized at a known Greenwich Mean Sidereal Time (GMST), typically zero. This alignment implies:

$$R_{\mathcal{R}}^{\mathcal{I}}(t = 0) = \mathbf{I}_{3\times3} \tag{6.6}$$

where $R_{\mathcal{R}}^{\mathcal{I}}$ is the rotation matrix from ECEF to ECI. This simplifies the initial attitude calculations and ensures consistent initialization across reference frames.

Angular Velocity Initialization The initial angular velocity of the satellite body is specified relative to the orbital frame:

$$\boldsymbol{\omega}_{\mathcal{B}/\mathcal{O}}^{\mathcal{B}} = \begin{bmatrix} \omega_x \\ \omega_y \\ \omega_z \end{bmatrix} \tag{6.7}$$

Since the ECI and ECEF frames are aligned at $t = 0$, and the orbital frame is defined in the ECI frame, this implies that the angular velocity of the body with respect to the inertial frame is initially equivalent to the angular velocity with respect to the orbital frame:

$$\boldsymbol{\omega}_{\mathcal{B}/\mathcal{I}}^{\mathcal{B}}(t = 0) = \boldsymbol{\omega}_{\mathcal{B}/\mathcal{O}}^{\mathcal{B}}(t = 0) \tag{6.8}$$

This relationship holds only at the initialization instant. As time progresses, the orbital frame rotates relative to the inertial frame due to the satellite's motion, and the distinction between $\boldsymbol{\omega}_{\mathcal{B}/\mathcal{I}}$ and $\boldsymbol{\omega}_{\mathcal{B}/\mathcal{O}}$ becomes significant and must be handled accordingly in the attitude propagation.

Chapter 7

Experiments

7.1 Introduction

7.2 Conclusion

Chapter 8

Conclusion and Future Work

8.1 Conclusion

8.2 Future Work

References

[1] W. C. de Jongh, “Space debris: Pose estimation using stereo vision,” 2019.

[2] G. J. J. Korf, “Pose estimation of space objects,” 2024.

[3] H. W. Jordaan, “Spinning solar sail: The deployment and control of a spinning solar sail satellite,” 2016.

[4] J. Diebel, “Representing attitude: Eular angles, unit quaternions, and rotation vectors,” 2006.

Appendix A

Appendix title goes here